# Variation in Photosynthetic Pathways

## *I. Overall patterns of the $C_3$ carboxylation cycle (PCR) - (Figure)*

- $C_3$ carboxylation cycle using ribulose-1,5-bisphosphate carboxylase (Rubisco) is found in all plants
- Rubisco catalyses the carboxylation and oxygenation of RuBP and because of the high amount of oxygen (21%) to carbon dioxide (~0.037%) in our atmosphere, carboxylation efficiency of Rubisco is poor (competitive inhibition by $O_2$); see last section on evolution
- Functional significance of oxygenase activity of Rubisco is poorly understood but appears it is an unavoidable product of the reaction mechanism for carboxylation (an inherent constraint) but is also linked to "recycling activities" for phosphoglycolate and for nitrate reduction in leaves

## *II. Mechanisms to improve carboxylation efficiency*

A. Increases in the $CO_2/O_2$ specificity of Rubisco (Figures)
- $CO_2/O_2$ specificity spans an order of magnitude in different organisms
- possible evolutionary modification of Rubisco?
- anaerobic organisms lowest $CO_2/O_2$ specificity
- $C_3$ plants highest specificity

B. $CO_2$ concentrating mechanisms (2 types)
- biochemical mechanisms - $C_4$ acid synthesis; eg. $C_4$ plants and CAM plants
- biophysical mechanisms - bicarbonate pump; e.g. many aquatic plants (see Bowes 1985, Raven et al. 1985)

## *III. Biochemical $CO_2$ concentrating mechanisms*

- initial fixation of atmospheric carbon by phosphoenol pyruvate (PEP) carboxylase
- initial formation of $C_4$ acid (malate, aspartate)
- decarboxylation of $C_4$ acid to produce $CO_2$ which is fixed in $C_3$ cycle

A. **$C_4$** photosynthetic pathway (Figures)

- spatial separation of RuBP carboxylase and PEP carboxylase is essential
- specialized morphology called **Kranz** anatomy (Figures)
- the PEPcase system acts as a $CO_2$ concentrating mechanism or "$CO_2$ pump" creating high $CO_2$ levels in the bundle sheath cells
- three $C_4$ variants do occur: NADP-ME; NAD-ME; PEP-CK (Figures)

B. **CAM** photosynthetic pathway (Figures)

- temporal separation of PEP and Rubisco activity
- succulent tissue with large vacuoles required for storage of acid overnight
- high $CO_2$ concentration created behind closed stomata during daylight period

## *IV. Benefits of biochemical $CO_2$ concentrating mechanisms*

A. Increased water-use efficiency **(WUE)**

**1. $C_4$ plants:**
- $C_4$ plants would have to have lower stomatal conductance to maintain equivalent photosynthetic rates as $C_3$ plants (Figure)

- $CO_2$ 'pump' results in different photosynthetic dependence on intercellular $CO_2$ in $C_4$ plants compared to $C_3$ plants (Figure)
- much lower intercellular $CO_2$ in $C_4$ plants (Figure) is always seen

**2. CAM plants:**
- stomatal opening mainly <u>at night</u> when temperature is lower and humidity is higher results in less water loss (Figure)

B. Increased nitrogen-use efficiency **(NUE)**

- in order to maintain the same photosynthetic rates, $C_4$ plants require less investment in RuBisco (a large, high nitrogen content protein; Figures)

## *V. Costs of biochemical $CO_2$ concentrating mechanisms*

- extra energy (ATP, NADPH) costs in both $C_4$ and CAM plants
- energy costs dependent on environmental conditions

A. **$C_4$ plants:**
- extra energy costs reflected in quantum yield requirements in $C_3$ and $C_4$
- $C_3$ quantum yield dependent on $CO_2$ concentration and temperature (Figure)
- $C_4$ quantum yield independent of $CO_2$ (or $O_2$) concentration and temperature (Figure)
- all else equal expect $C_4$ plants to be most efficient and abundant in hot, dry, high light habitats (Figures, and last section)
- $C_4$ plants also occur in cool environments and aquatic environments high NUE may be beneficial in aquatic habitats

B. **CAM plants:**
- CAM well adapted to hot, dry environments, high WUE
- CAM plants can be adapted to aquatic environments
- uptake of $CO_2$ at night when $CO_2$ is most readily available in vernal pools
- trade-off of desiccation or starvation (Figures)
- 50% of all CAM plants are epiphytes
- $CO_2$ acquisition at night provides competitive advantage (Figure)
- high energy costs and low $CO_2$ assimilation rates result in low productivity

## *VI. Shifts in photosynthetic pathway*

A. $C_3$ - CAM shifts dependent on water availability or salinity (Figure)
B. CAM epiphyte shifts to $C_3$ when rooted on ground (eg. *Clusia*)
C. *Frerea* has deciduous $C_3$ leaves and CAM stems (Figure)
D. *Eleocharis* (an aquatic plant) has $C_4$ terrestrial leaves, $C_3$ submerged leaves
E. *Isoetes* has CAM leaves when submerged, $C_3$ leaves when emergent

## *VII. The evolution of $C_3$, $C_4$, and CAM photosynthesis: paleo-evidence and phylogenetic patterns*

A. $C_3$ pathway present in all phyla and orders - most widespread photosynthetic syndrome

B. $C_4$ present only in angiosperms; available data suggest multiple, independent evolutionary origins (Figure, Table)

C. CAM present in ferns, gymnosperms, and angiosperms; independent evolutionary origins probably also occurred (Table)

D. $C_3$ and $C_4$ appear in a single genus several times (Table)

- $C_4$ pathway is clearly a $CO_2$ concentrating mechanism - Did it evolve in response to low $[CO_2]$

or high aridity (?) ==- Look at Paleo-evidence (Figures)

E. Changes in ambient $[CO_2]$ and the ratio of photorespiration to photosynthesis may have been more important than aridity in the evolution of $C_4$ photosynthesis (Figures) - but -

F. Broad pattens may depend upon if a species is a moncot or dicot (Figures)

---

**Table A.** Genera which have been shown to possess **both $C_3$ and $C_4$ species**

see Also: Sage & Monson (1999).

| Family | Genus |
|---|---|
| Aizoaceae | Mollugo |
| Amaranthaceae | Aerva<br>Alteranthera |
| Boraginaceae | Heliotropium |
| Chenopodiaceae | Atriplex<br>Bassia<br>Kochia<br>Suaeda |
| Compositae | Flaveria<br>Pectis |
| Cyperaceae | Cyperus<br>Scirpus |
| Euphorbiaceae | Chamaesyce<br>Euphorbia |
| Gramineae | Alloteropsis<br>Panicum |
| Nyctaginaceae | Boerhaavia |
| Zygophyllaceae | Kallstroemia<br>Zygophyllum |

**Table B.** Plant families known to possess the **$C_4$ photosynthetic pathway** (also see Table 1 from Ehleringer et al., 1997 below).

| | |
|---|---|
| Acanthaeceae | |
| Aizoaceae | Cyperaceae |
| Amaranthaceae | Euphorbiaeceae |
| Boraginaceae | Gramineae |
| Capparidaceae | Nyctaginaceae |
| Caryophyllaceae | Polygonaceae |
| Chenopodiaceae | Portulacaceae |
| Cleomaceae | Scrophulariaceae |
| Compositae | Zygophyllaceae |

Table C. Plant families known to possess the Crassulacean Acid Metabolism **(CAM)** pathway.

| | |
|---|---|
| Polypodiales | Polypodiaceae (ferns) |
| Gymnospermae | Welwitschiaceae |
| Monocotyledonae | Agavaceae |
| | Bromeliaceae |
| | Liliaceae |
| | Orchidaceae |
| Dicotyledonae | Aizoaceae |
| | Asclepiadaceae |
| | Bataceae |
| | Cactaceae |
| | Capparidaceae |
| | Caryophyllaceae |
| | Chenopodiaceae |
| | Compositae |
| | Crassulaceae |
| | Cucurbitaceae |
| | Didiereaceae |
| | Euphorbiaceae |
| | Geraniaceae |
| | Labiatae |
| | Oxalidaceae |
| | Passifloraceae |
| | Piperaceae |
| | Plantaginaceae |
| | Portulacaceae |
| | Tetragoniaceae |
| | Vitaceae |
| | ? - other unknown desert families |

## LITERATURE

Bowes, G. 1985. The pathways of $CO_2$ fixation by aquatic organisms. In: Inorganic carbon uptake by aquatic photosynthetic organisms. Edited W.J. Lucus and J.A. Berry. American Society of Plant Physiologists, Rockville, MA.

Brown, R.H. 1978. A difference in N-use efficiency in $C_3$ and $C_4$ plants and its implications in adaptation and evolution. Crop Sci. 18:93-98.

Brown, W.V. and B.N. Smith. 1972. Grass evolution, the Kranz syndrome. $^{13}C/^{12}C$ ratios, and continental drift. Nature 239:345-346.

Burris, R.H. and C.C. Black (eds.). 1975. $CO_2$ metabolism and plant productivity. University Park Press, Baltimore.

Cerling, T.E. et al. 1997. Global vegetation change through the Miocene/Pliocene boundary. Nature 389: 153-158.

Cerling, T.E., Y. Wang, and J. Quade. 1993. Expansion of $C_4$ ecosystems as an indicator of global ecological change in the late Miocene. Nature 361: 344-345.

Ehleringer, J.R. and O. Björkman. 1977. Quantum yields for $CO_2$ uptake in $C_3$ and $C_4$ plants: dependence on temperature, $CO_2$, and $O_2$ concentrations. Plant Physiol. 59:86-90.

Ehleringer, J.R. 1978. Implications of quantum yield differences on the distributions of $C_3$ and $C_4$ grasses. Oecologia 31:255-267.

Ehleringer, J. 1979. Photosynthesis and photorespiration: biochemistry, physiology, and ecological implications. Hortscience 14:217-221.

Ehleringer, J.R., and R.W. Pearcy. 1983. Variation in quantum yield for $CO_2$ uptake among $C_3$ and $C_4$ plants. Plant Physiol. 73:555-559.

Ehleringer, J.R., R.F. Sage, L.B. Flanagan and R.W. Pearcy. 1991. Climate change and the evolution of $C_4$ photosynthesis. Trends in Ecology and Evolution 6: 95-99.

Ehleringer, J.R. and R. K. Monson. 1993. Evolutionary and Ecological Aspects of Photosynthetic Pathway Variation. Ann. Rev. of Ecology and Systematics 24: 411-439

Ehleringer, J.R., T.E. Cerling, and B.R. Helliker. 1997. $C_4$ photosynthesis, atmospheric $CO_2$, and climate. Oecologia 112: 285-299.

Epstein H.E. et al. 1997. Productivity patterns of C3 and C4 functional types in the U.s. Great Plains. Ecology 78: 722-731.

Griffiths, H. 1990. Carbon dioxide concentrating mechanisms and the evolution of CAM in vascular epiphytes. In: Vascular plants as epiphytes. Ecological studies 76. Edited U. Luttge. Springer-Verlag, Berlin.

Griffiths, H. 1988. Crassulacean acid metabolism: a reappraisal of physiological plasticity in form and function. Advances in Botanical Research 15: 43-92.

Hatch, M.D. 1988. C4 photosynthesis: a unique blend of modified biochemistry, anatomy and ultrastructure. Biochimica et Biophysica Acta 895: 81-106

Hatch, M.D. and C.R. Slack. 1966. Photosynthesis by sugarcane leaves. A new carboxylation reaction and the pathway of sugar formation. Biochem. J. 101:103-111.

Hatsock, T.L. and P.S. Nobel. 1976. Watering converts a CAM plant to daytime $CO_2$ uptake. Nature 262:574-576.

Kortschak, H.P., C.E. Hart, and G.O. Burr. 1965. Carbon dioxide fixation in sugarcane leaves. Plant Physiol. 40:209-213.

Lange, O. and M. Zuber. 1977. *Frerea indica*, a stem succulent CAM plant with deciduous $C_3$ leaves. Oecologia 31:67-72.

Monson, R.K. 1989. On the evolutionary pathways resulting in $C_4$ photosynthesis and CAM. Advances in Ecological Research 19:57-110.

Monson, R.K. 1989. On the significance of $C_3$-$C_4$ intermediate photosynthesis to the evolution of $C_4$ photosynthesis. Plant, Cell and Environment 12: 689-699.

Morgan, M.E., J.D. Kingston, and B.D. Marino. 1994. Carbon isotope evidence for the emergence of $C_4$ plants in the Neogene from Pakistan and Kenya. Nature 367: 162-165.

Nambudiri, E.M.V., W.D. Tidwell, B.N. Smith, and N.P. Hebbert. 1978. A $C_4$ plant from the Pliocene. Nature 276:816-817.

Ogren, W.L. and G. Bowes. 1971. Ribulose diphosphate carboxylase regulates soybean photorespiration. Nature 230:159-160.

Osmond, C.B., Winter, K. and Ziegler, H. 1982. Functional significance of different pathways of photosynthesis. In: Encyc. of Plant Physiology, New Series Vol. 12B pp. 479-547, Springer-Verlag, Berlin

Pearcy, R.W., and J.R. Ehleringer. 1984. Comparative ecophysiology of $C_3$ and $C_4$ plants. Plant Cell Environ. 7:1-13.

Quade, J, T.E. Cerling, and J.R. Bowman. 1989. Development of Asian Monsoon revealed by marked ecological shift during the latest Miocene in northern Pakistan. Nature 342: 163-166.

Raven, J.A., B.A. Osborne and A.M. Johnson. 1985. Uptake of CO2 by aquatic vegetation. Plant Cell Environ. 8:417-425.

Sage, R.F. and R. K. Monson. 1999. $C_4$ Plant Biology. Academic Press, San Diego, CA

Sage, R. and R.W. Pearcy. 1987. The nitrogen-use efficiency of $C_3$ and $C_4$ plants. Plant Physiol. 84: 954-967.

Stowe, L.G. and J.A. Teeri. 1978. The geographic distribution of $C_4$ species of the Dicotylendonae in relation to climate. Amer. Nat. 112:609-623.

Teeri, J.A. and L.G. Stowe. 1976. Climatic patterns and the distribution of $C_4$ grasses in North America. Oecologia 23:1-12.

Teeri, J.A., L.G. Stowe, and D.A. Murawski. 1978. The climatology of two succulent plant families: Cactaceae and Crassulaceae. Can. J. Bot. 56:1750-1758.

Ueno, O., Samejima, M., Muto, S. and Miyachi, S. 1988. Photosynthetic characteristics of an amphibious plant, *Eleocharis vivipara*: Expression of $C_4$ and $C_3$ modes in contrasting environments. Proc. Natl. Acad. Sci. 85: 6733-6737.

Vogel, J.C. 1993. Variability of carbon isotope fractionation during photosynthesis. Pp. 29-46 In: J.R. Ehleringer, A.E. Hall and G.D. Farquhar (eds). *Stable Isotopes and Plant Carbon-Water Relations*. Academic Press, San Diego.

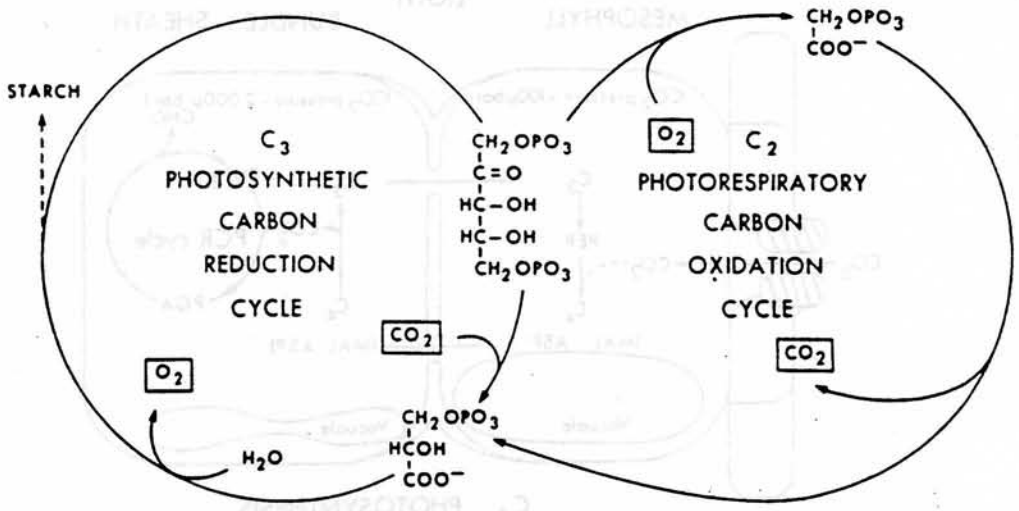


Fig. 15.1. Linkage of the photosynthetic carbon reduction cycle and the photorespiratory carbon oxidation cycle by $RuP_2$ carboxylase-oxygenase and its reaction products

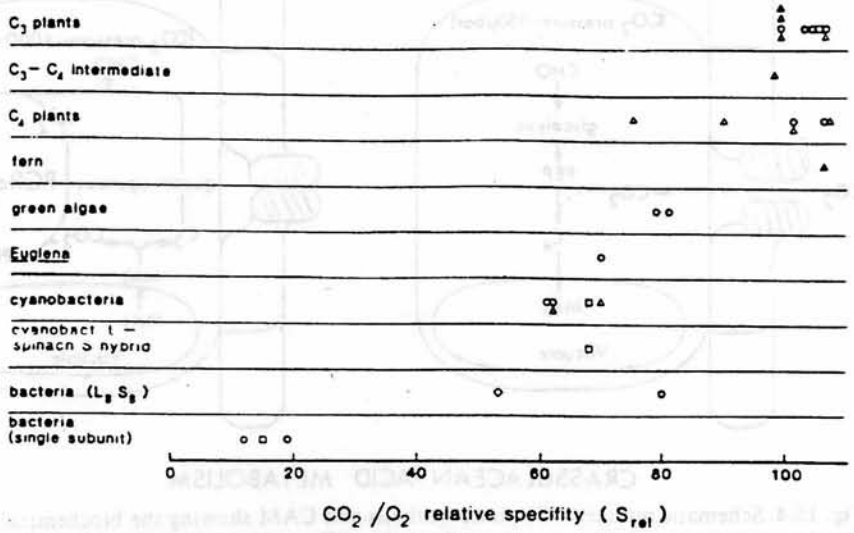


Fig. 3. The relative specificity ($s_{rel}$) scale; $s_{rel} = [V_c/K_c]/[V_o/K_o]$. Data were taken from: ○, Jordan and Ogren (1981); △, Jordan and Ogren (1983); □, Andrews and Lorimer (1985); ◇, Jordan and Chollet (1985). The $s_{rel}$ values from different laboratories vary according to the p$K'$ assumed for the $CO_2 \leftrightarrow HCO_3^-$ equilibrium. This p$K'$ decreases linearly with the logarithm of ionic strength and thus becomes relatively insensitive to ionic strength above ionic strength 0.1. Ionic strengths of approximately 0.1 and above are usual in most carboxylase assay buffers. Therefore, we have recalculated published $s_{rel}$ values in accordance with a p$K'$ of 6.12, which is the value appropriate to an ionic strength of 0.1 at 25°C (Yokota and Kitaoka, 1985).

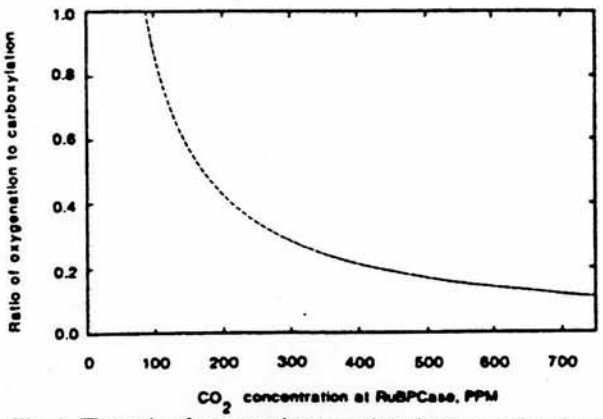


Fig. 1. The ratio of oxygenation to carboxylation as a function of $CO_2$ concentration at the site of carboxylation. The data are calculated for $C_3$ type RuBPcase at 25°C using the value for gamma star ($\Gamma$.) from Brooks and Farquhar 1985).

Lecture Topic 9 - Figures

Figures for: Photosynthetic Pathway Variation

1

separation of activities in space

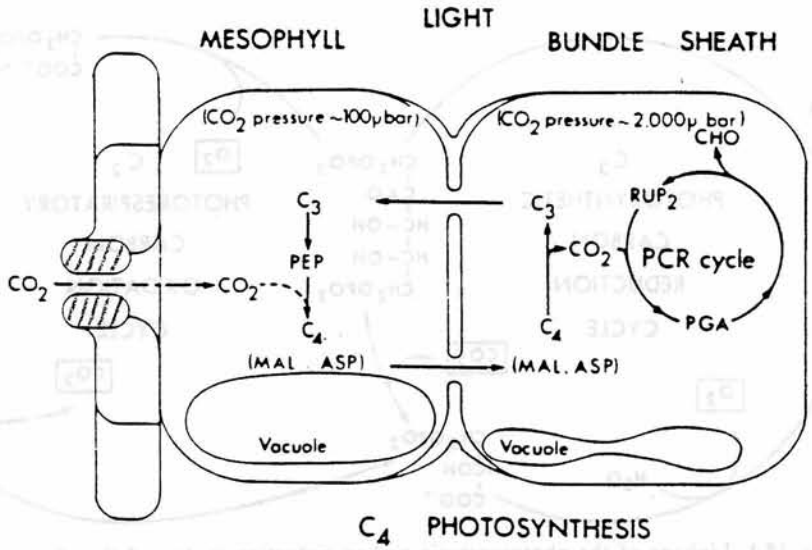


$C_4$ PHOTOSYNTHESIS

separation of activities in time

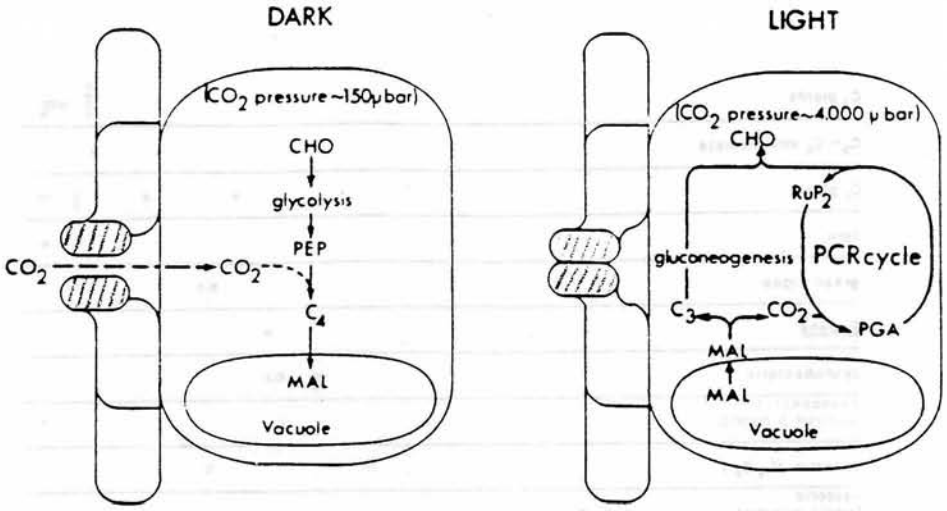


CRASSULACEAN ACID METABOLISM

**Fig. 15.4.** Schematic outline of $C_4$ photosynthesis and CAM showing the biochemical analogies between the two pathways, as well as the differences in spatial ($C_4$) and temporal (CAM) organization of the component processes. (After BJÖRKMAN 1973)

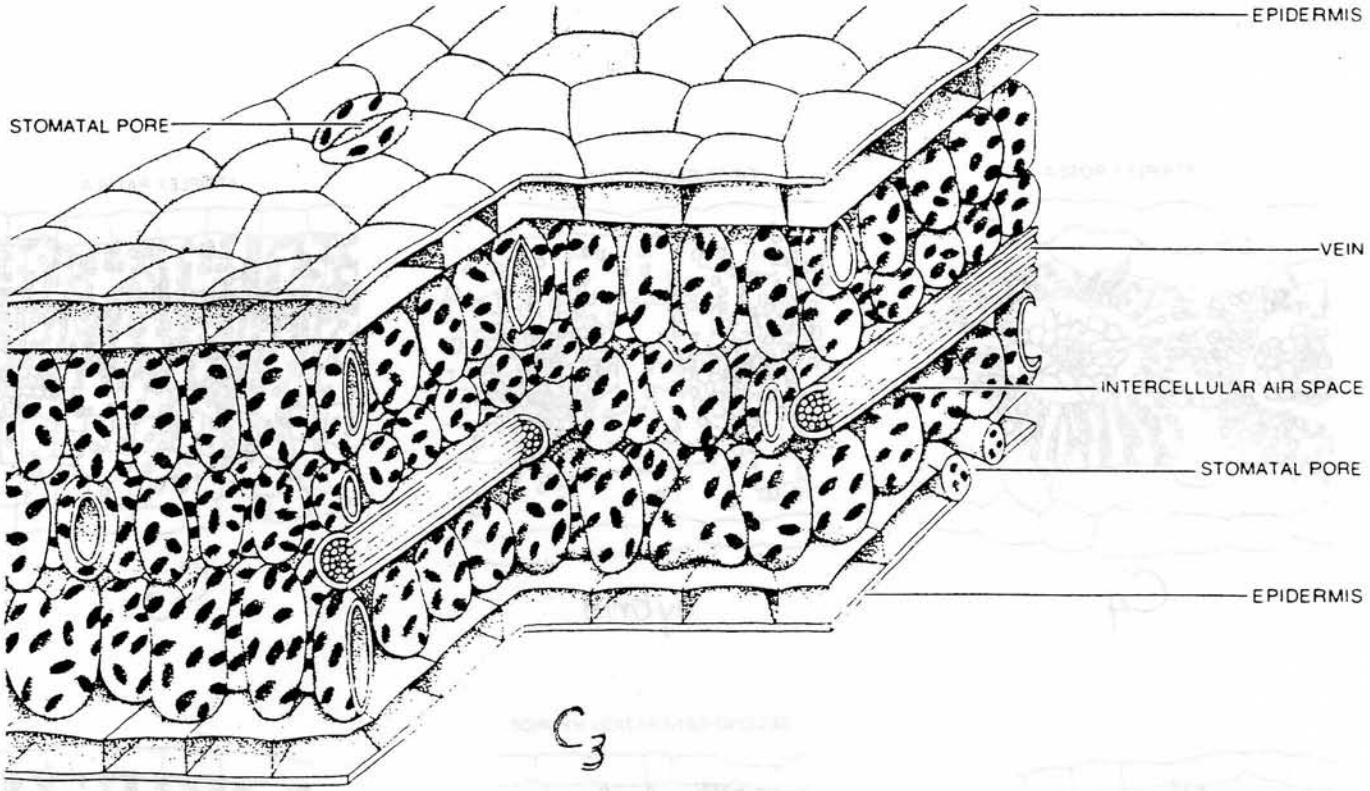


LEAF STRUCTURE of the three-carbon plant *Atriplex patula* is portrayed. As in other typical leaves the cells, containing chlorophyll, which is shown in color, are of a single type, and they are found throughout the interior of the leaf. *A. patula* has a relative, *A. rosea*, that employs the four-carbon pathway for photosynthesis and has a different leaf structure, shown in the illustration below.

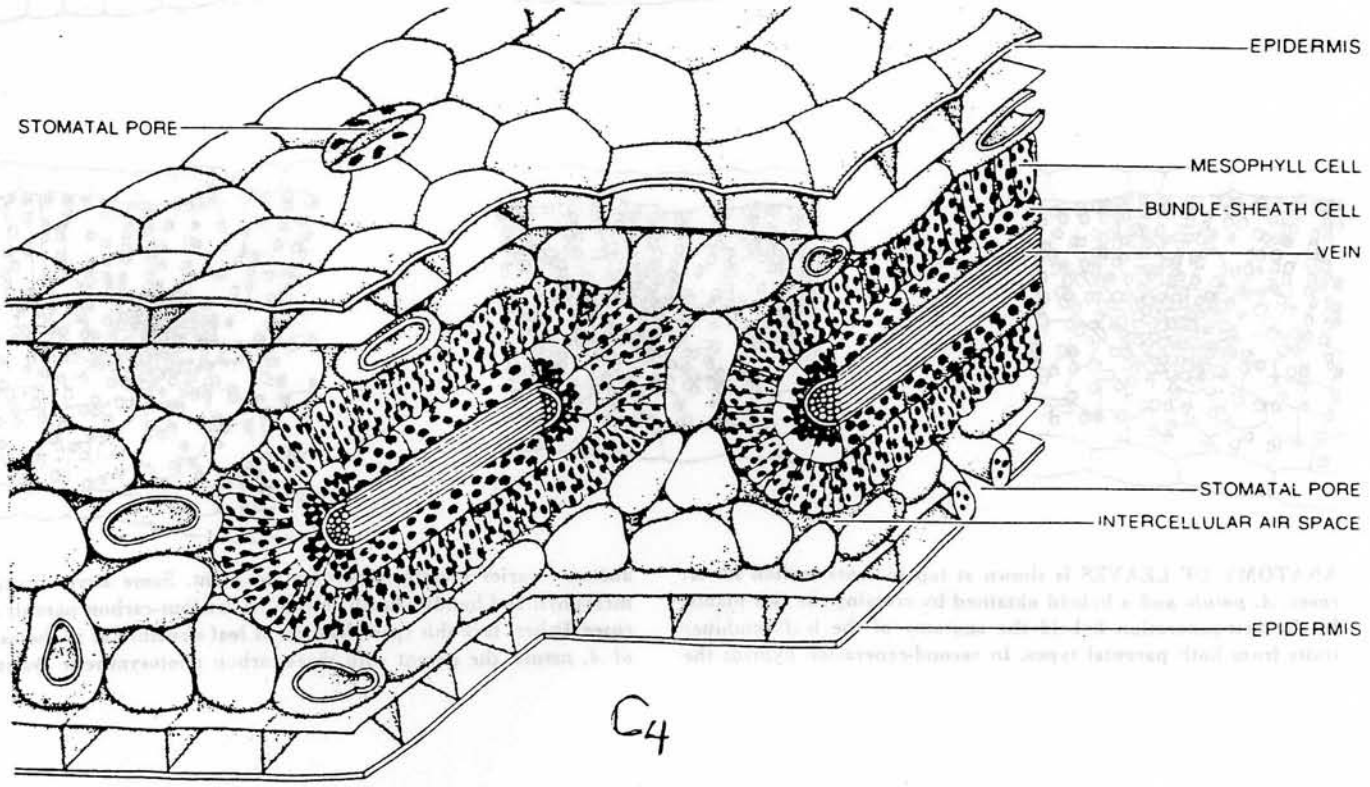


SPECIALIZED LEAF of *A. rosea* has nearly all its chlorophyll in two types of cells, which form concentric cylinders around the fine veins of the leaf. The cells of the outer cylinder are mesophyll cells; those of the inner cylinder are bundle-sheath cells.

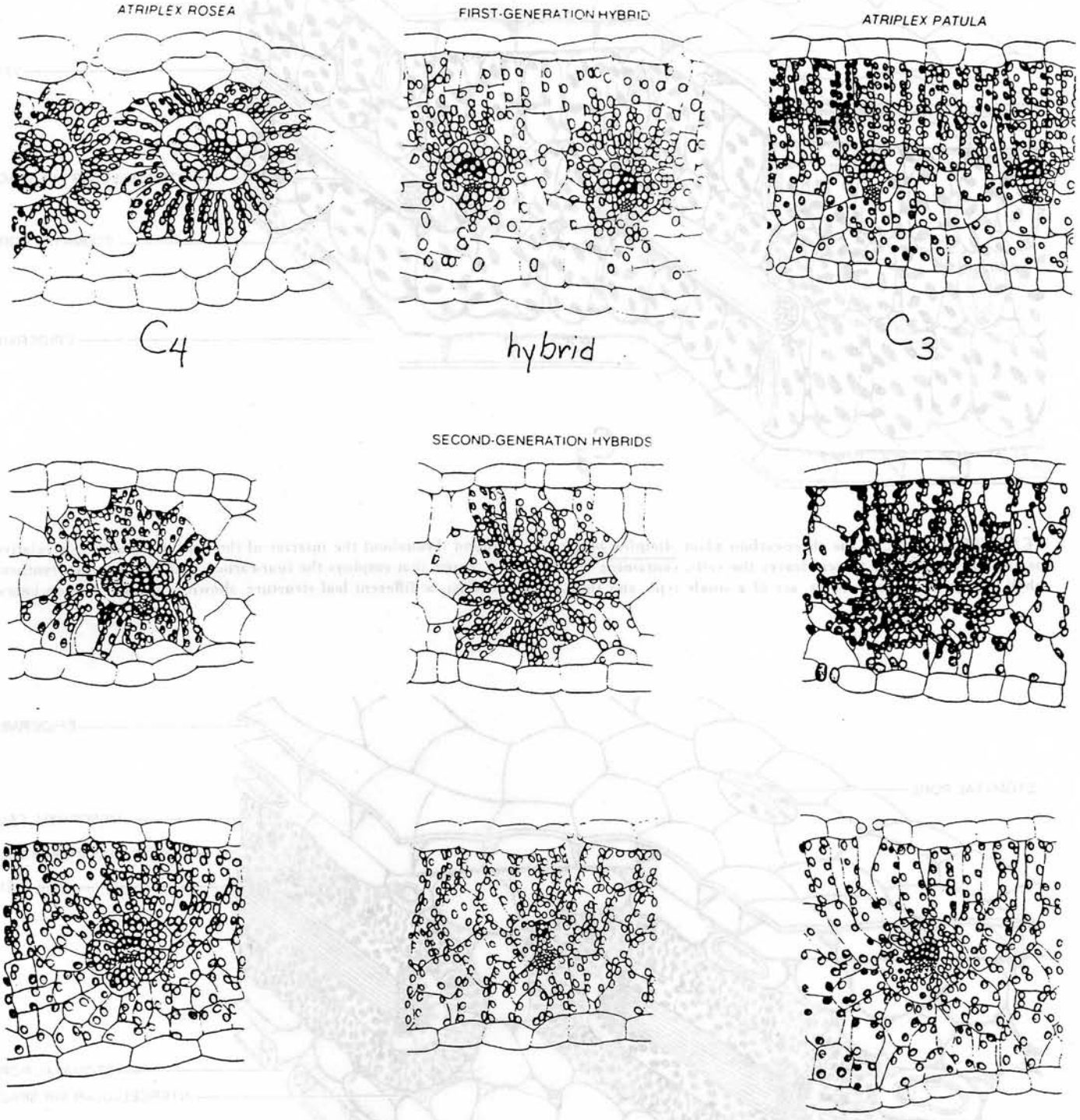


ANATOMY OF LEAVES is shown at top in cross section for *A. rosea*, *A. patula* and a hybrid obtained by crossing the two plants. In the first-generation hybrid the anatomy of the leaf combines traits from both parental types. In second-generation hybrids the anatomy varies greatly from plant to plant. Some have distinct mesophyll and bundle-sheath cells as in the four-carbon parent, *A. rosea*. Others lack this specialization of leaf structure as in the case of *A. patula*, the parent with three-carbon photosynthetic system.

**TABLE 9.4.** Three variants of the C4 photosynthetic carbon assimilation cycle

| *Principal C4 acid transported to the bundle sheath cells* | *Decarboxylating enzyme* | *Variant name* | *Principal C3 acid returned to mesophyll cells* | *Examples* |
|---|---|---|---|---|
| Malate | NADP-dependent malic enzyme (chloroplast) | NADP-ME | Pyruvate | Maize, crabgrass sugarcane, sorghum |
| Aspartate | NAD-dependent malic enzyme (mitochondria) | NAD-ME | Alanine | Millet, pigweed (*Panicum miliaceum*) |
| Aspartate | Phosphoenolpyruvate carboxykinase (cytoplasm) | PEP-CK | Alanine/pyruvate | Guinea grass (*Panicum maximum*) |

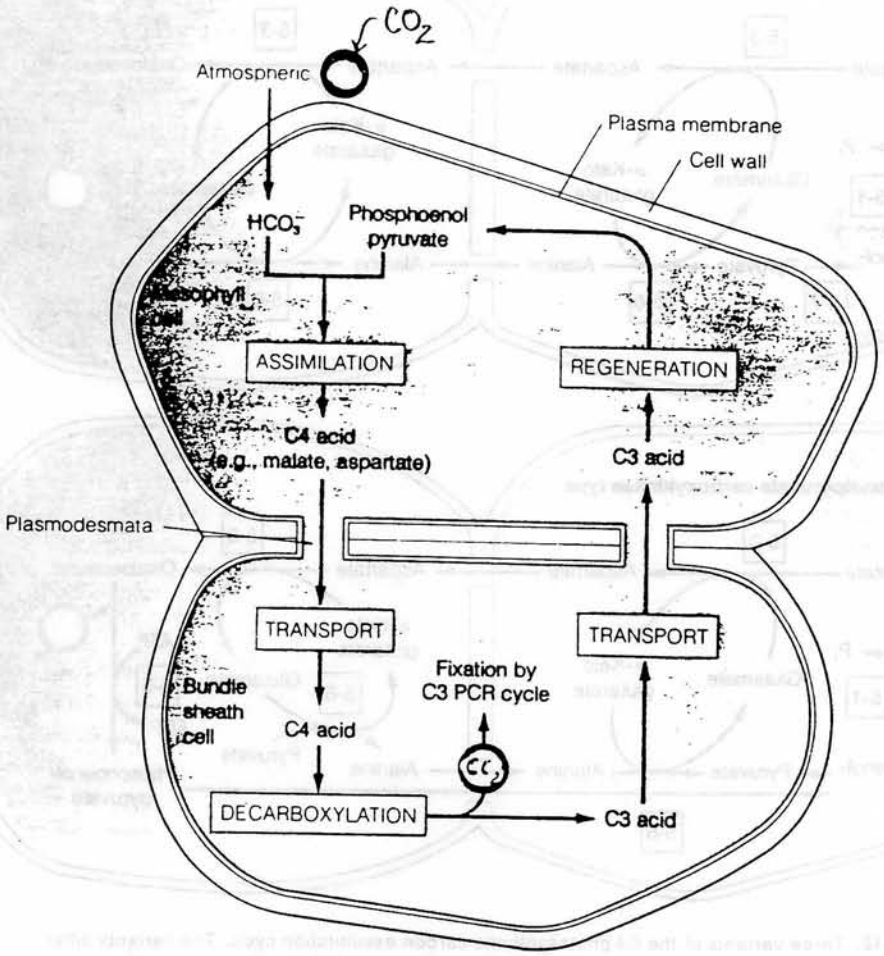


**FIGURE 9.11.** The basic C4 photosynthetic carbon assimilation cycle involves two cell types and proceeds in four stages: *assimilation* of $CO_2$ and its incorporation into a four-carbon acid in the mesophyll cells; *transport* of the four-carbon acid from the mesophyll cells to the bundle sheath cells; *decarboxylation* of the four-carbon acid, generating a high concentration of $CO_2$ in the bundle sheath cells; and *transport* of a three-carbon acid back to the mesophyll cells, where the original $CO_2$ acceptor, phosphoenolpyruvate, is regenerated. The C4 PCA cycle effectively concentrates $CO_2$ in the bundle sheath cells, to which Rubisco and the other enzymes of the C3 PCR cycle are restricted. This high concentration of $CO_2$ in the bundle sheath cells effectively suppresses oxygenation via the C2 PCO cycle.

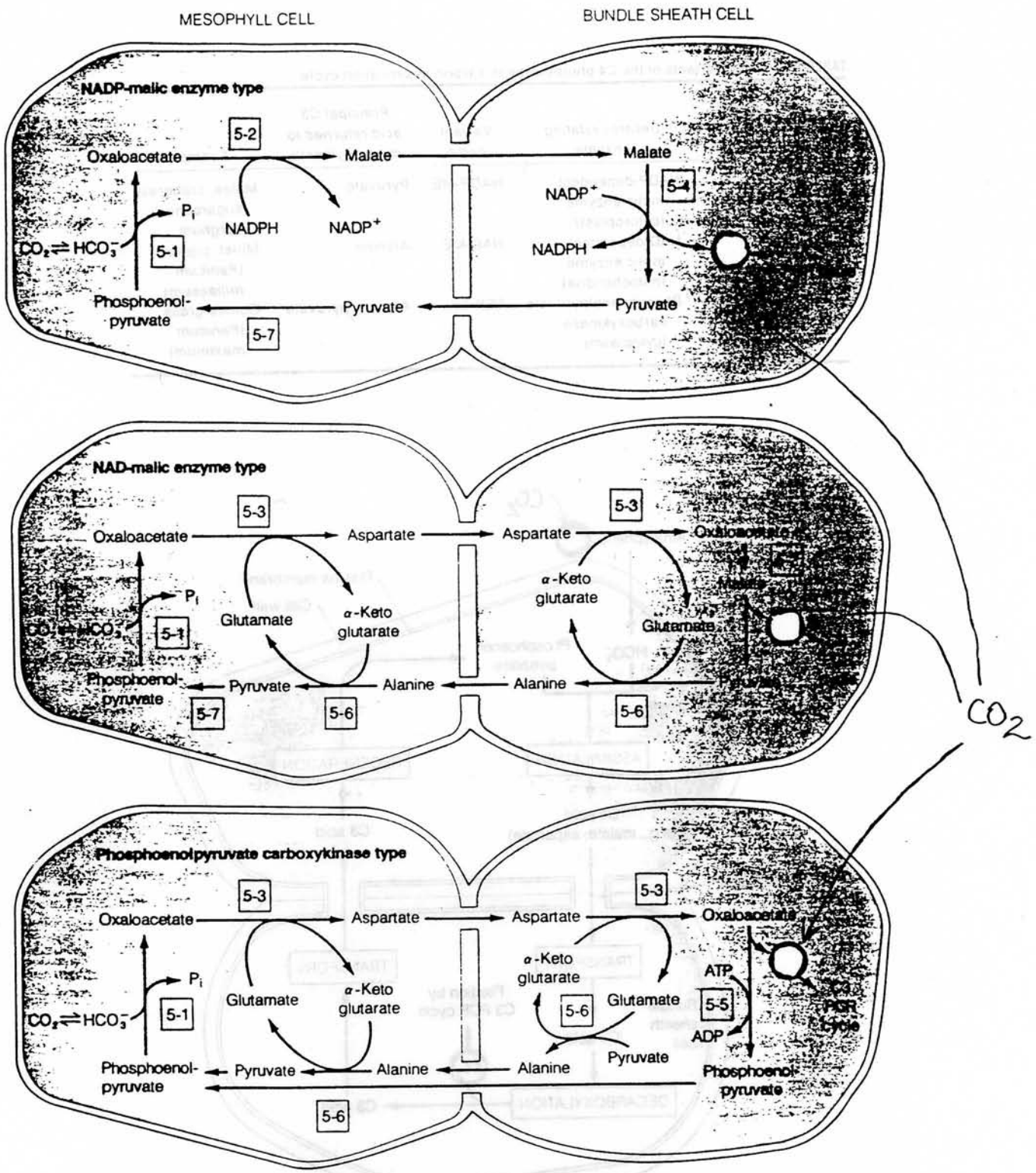


**FIGURE 9.12.** Three variants of the C4 photosynthetic carbon assimilation cycle. The variants differ principally in (1) the nature of the four-carbon acid (malate or aspartate) transported into the bundle sheath cell and of the three-carbon-acid (pyruvate or alanine) returned to the mesophyll cell and (2) the nature of the enzyme catalyzing the decarboxylation step in the bundle sheath cell. The three variants are named after the decarboxylation mechanism. The reactions (5-1, 5-2, etc.) are more fully described in Table 9.5. Within a mesophyll cell or a bundle sheath cell, different reactions can occur in different compartments, such as the cytosol, the mitochondrion, or the chloroplast.

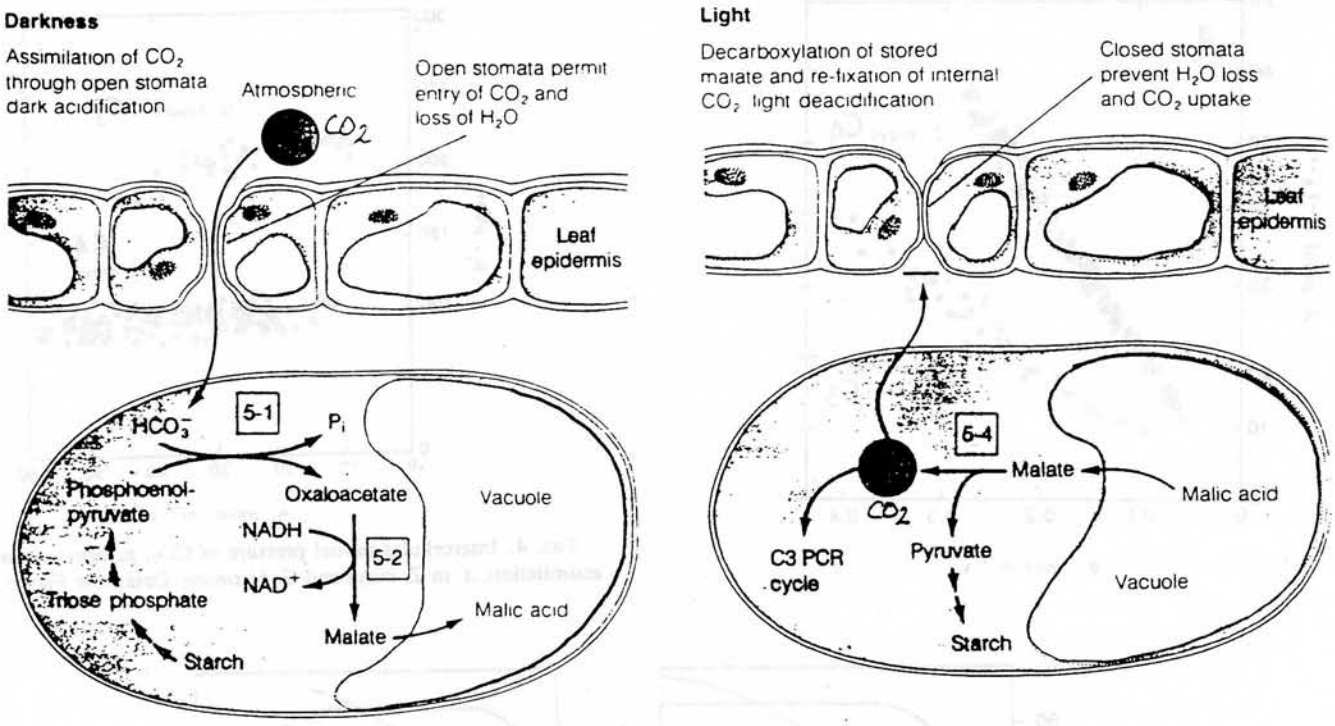


**FIGURE 9.14.** Crassulacean acid metabolism (CAM) involves the temporal separation of $CO_2$ assimilation at night and decarboxylation and refixation of the internally released $CO_2$ during day. CAM is primarily an adaptation to minimize the loss of water that occurs whenever stomata are opened to permit the entry of $CO_2$. In CAM plants, the stomata are opened in the cool of the night. $CO_2$ is assimilated as malic acid, which is stored in the vacuole. As malic acid accumulates, the leaf vacuoles undergo dark acidification. Upon illumination, the stomata close, and the leaf deacidifies. The malic acid is recovered from the vacuole and undergoes decarboxylation. The $CO_2$ that is released is prevented from escaping by stomatal closure and is fixed via the C3 PCR cycle, using photochemically generated ATP and NADPH.

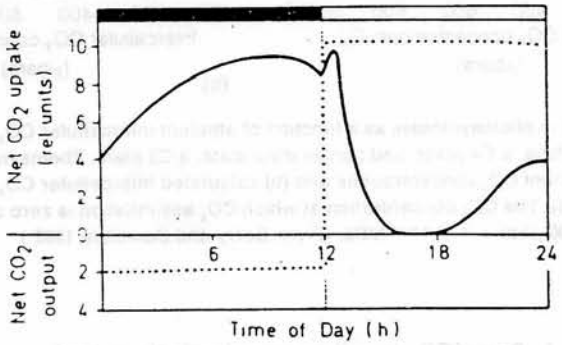


Fig. 5.1. Schematic standard curves of $CO_2$ exchange in a CAM plant (——) and a $C_3$ plant (·····)

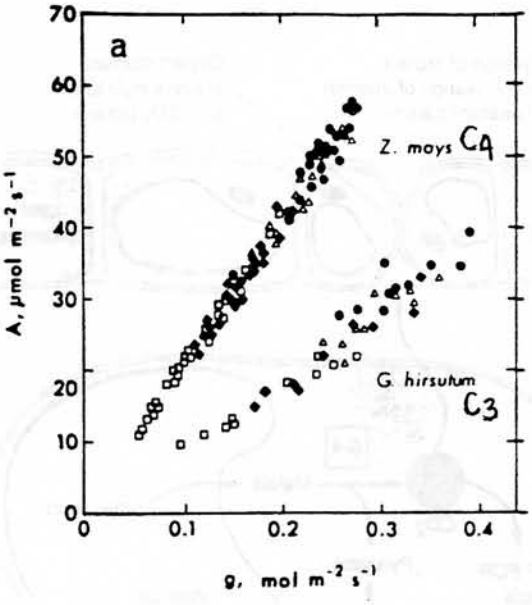


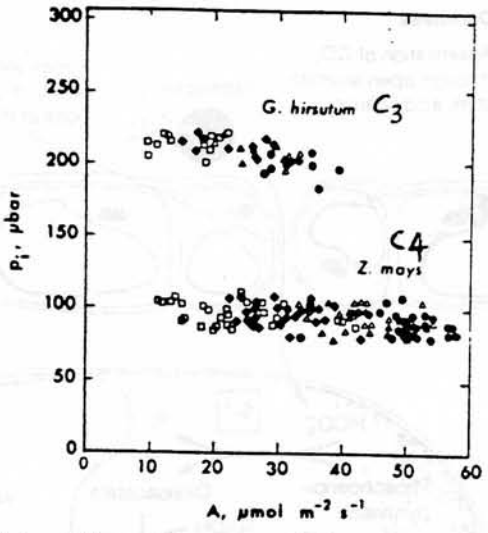


FIG. 4. Intercellular partial pressure of $CO_2$, $p_i$, against rate of $CO_2$ assimilation, $A$, in *Z. mays* and *G. hirsutum*. Data from Figure 3(a).

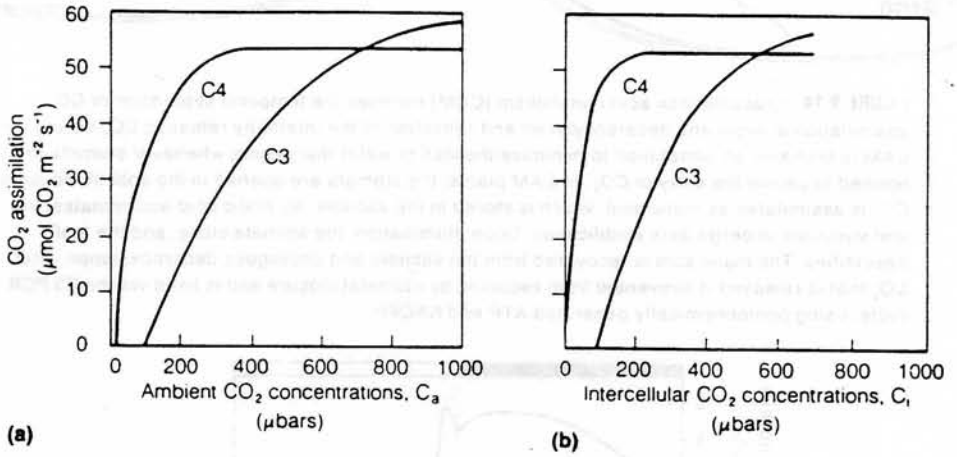


**FIGURE 10.10.** Changes in photosynthesis as a function of ambient intercellular $CO_2$ concentrations in *Tidestromia oblongifolia*, a C4 plant, and *Larrea divaricata*, a C3 plant. Photosynthetic rates are plotted against (a) ambient $CO_2$ concentrations and (b) calculated intercellular $CO_2$ concentrations inside the leaf (Eq. 10.5). The $CO_2$ concentration at which $CO_2$ assimilation is zero defines the $CO_2$ compensation point. 100 μbar = 1 × $10^{-3}$ MPa. (From Berry and Downton, 1982.)

Table 1. *Rate of $CO_2$ Assimilation (μmol $m^{-2}$ $s^{-1}$), A, Leaf Conductance to $CO_2$ Transfer (mol $m^{-2}$ $s^{-1}$), g, and Intercellular Partial Pressure of $CO_2$ (μbar), $p_i$, Measured with 2 mmol $m^{-2}$ $s^{-1}$ Photon Flux Density at the Illuminated Surface, 305 μbar Ambient Partial Pressure of $CO_2$, 30°C Leaf Temperature, and 20 mbar Vapor Pressure Difference between Leaf and Air*

| | A | g | $p_i$ |
|---|---|---|---|
| $C_3$ species | | | |
| *Atriplex hastata* | 29.8 | 0.35 | 225 |
| *Eucalyptus camaldulensis* | 35.4 | 0.32 | 201 |
| *Eucalyptus pauciflora* | 26.0 | 0.29 | 228 |
| *Gossypium hirsutum* | 33.0 | 0.35 | 216 |
| *Helianthus annuus* | 26.7 | 0.35 | 235 |
| *Phaseolus vulgaris* | 23.0 | 0.26 | 228 |
| *Rumex acetosa* | 14.0 | 0.12 | 194 |
| *Spinacia oleracia* | 22.2 | 0.20 | 196 |
| $C_4$ species | | | |
| *Amaranthus edulus* | 34.0 | 0.16 | 96 |
| *Imperata cylindrica* | 20.3 | 0.09 | 88 |
| *Pennisetum purpureum* | 55.7 | 0.26 | 98 |
| *Zea mays* | 53.0 | 0.25 | 94 |

INSTANTANEOUS WATER USE EFFICIENCY ($A/E$) FOR NET $CO_2$ ASSIMILATION OF SPECIES EXHIBITING DIFFERENT PHOTOSYNTHETIC PATHWAYS

| Species | Photoperiod | $A/E$ (mmol $CO_2$/mol $H_2O$) |
|---|---|---|
| *Gossypium hirsutum* ($C_3$) | light | 3.4 |
| *Zea mays* ($C_4$) | light | 6.7 |
| *Opuntia inermis* (CAM) | dark | 10.0 |
| *Opuntia inermis* (CAM) | light | 5.0 |

Measurements refer to a $\Delta W$ of 20 mbar. Tissue temperatures: 30 °C for *G. hirsutum* and *Z. mays*, unspecified for *O. inermis*. Data were taken from Wong (1979) and Osmond et al. (1979b).

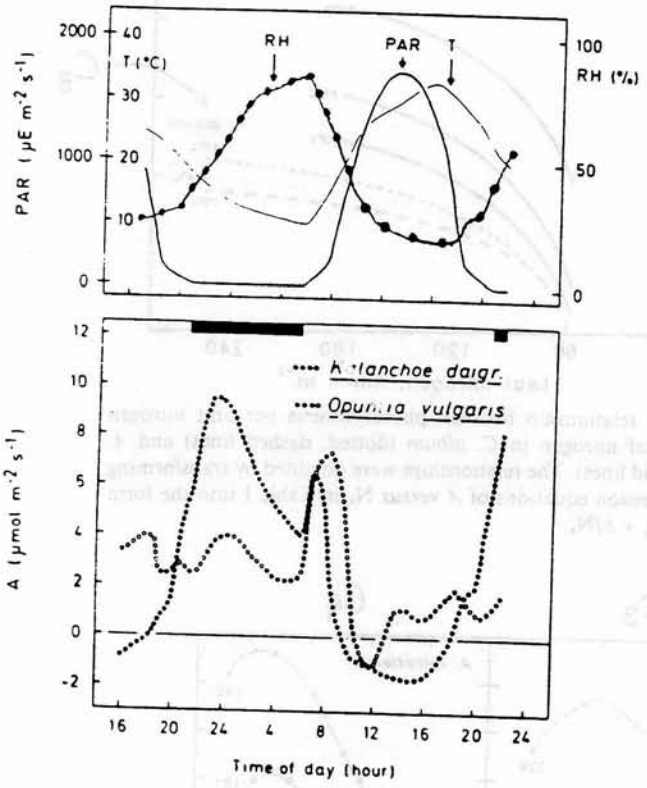


Fig. 8.4. Daily time course of PAR, ambient temperature ($T$), ambient relative air humidity (RH) and net $CO_2$ assimilation ($A$) of a leaf of *Kalanchoe daigremontiana* and a cladode (horizontally oriented) of *Opuntia vulgaris* in the Würzburg Botanic Garden on July 21/22, 1983. Ambient temperature and relative air humidity were automatically tracked inside the gas exchange cuvette. Plants were well watered and had been pre-conditioned for 3 weeks to the high light and temperature conditions prevailing during this particular summer period. (Winter and Meyer, unpublished.)

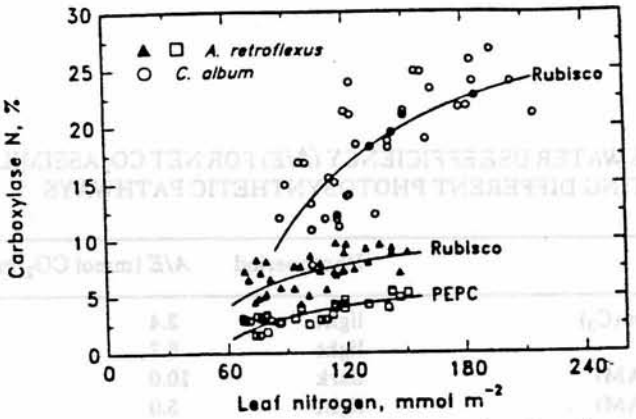


FIG. 4. Percent of leaf nitrogen in Rubisco as a function of organic leaf nitrogen in *C. album* (○) and *A. retroflexus* (▲), and the percent of leaf nitrogen in PEPC as a function of organic leaf nitrogen in *A. retroflexus* (□). The fitted curves represent the responses calculated by transforming the respective linear regressions of carboxylase content *versus* $N_o$ into the form of equation 2, and assuming that carboxylase protein is 16% N.

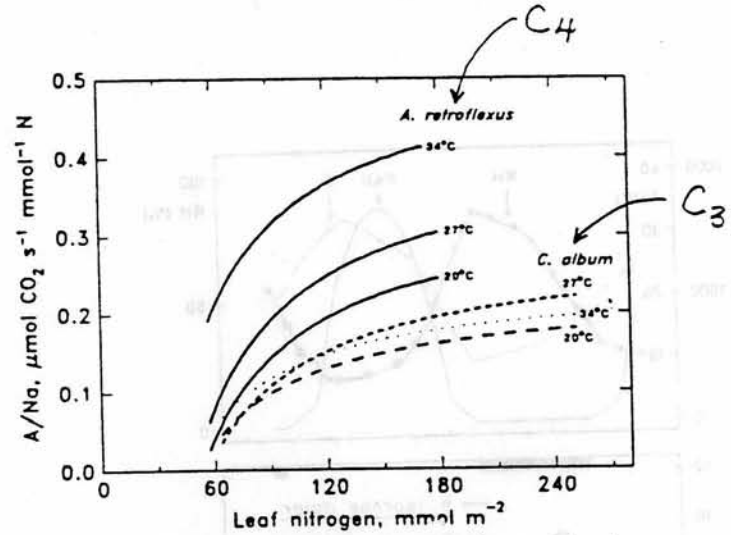


FIG. 2. The relationship between photosynthesis per unit nitrogen and organic leaf nitrogen in *C. album* (dotted, dashed lines) and *A. retroflexus* (solid lines). The relationships were obtained by transforming the linear regression equations of *A versus* $N_o$ in Table I into the form $A/N = dA/dN_o + b/N_o$.

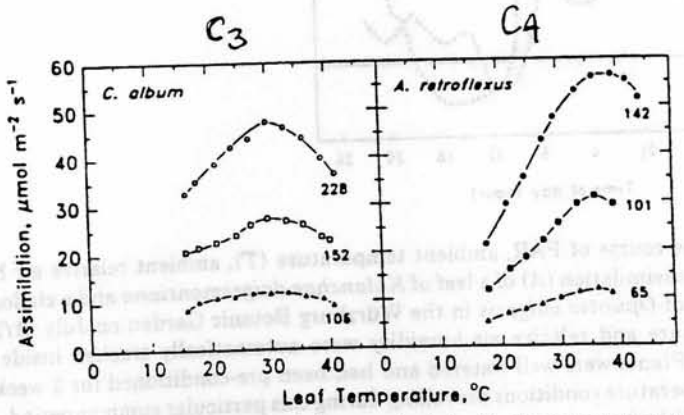


FIG. 5. The temperature of photosynthesis in *C. album* and *A. retroflexus* at light saturation. The values beside each curve represent organic leaf nitrogen content in mmol m$^{-2}$.

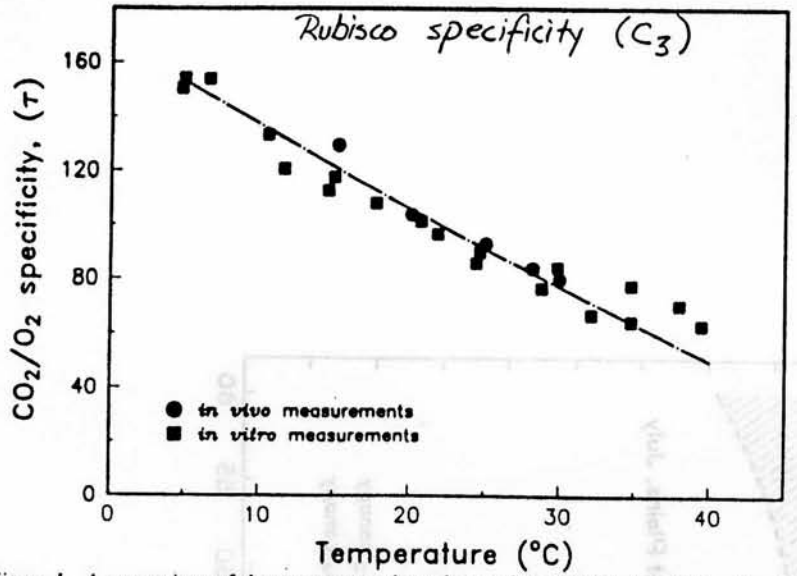


*Figure 1* A comparison of the temperature dependence of the $CO_2/O_2$ specificity of spinach Rubisco. Values were obtained from measurements of the $CO_2$-compensation point ($\Gamma^*$) of intact leaves by Brooks & Farquhar (22) and from simultaneous determination of RuBP-carboxylase and RuBP-oxygenase activities with purified spinach Rubisco in vitro by Jordan & Ogren (128). The dashed line is drawn using the $Q_{10}$=0.74 (Table 1).

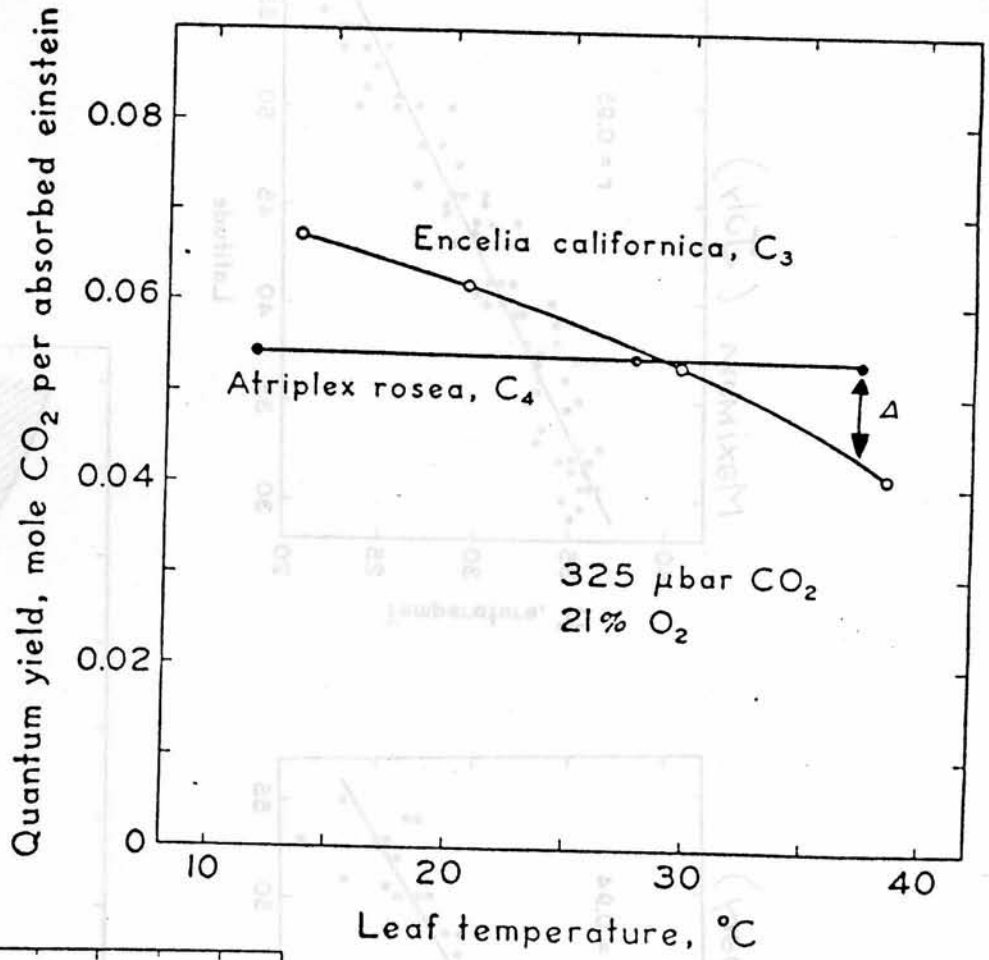


$\Delta$ = the change due to $CO_2/O_2$ specificity of Rubisco in $C_3$ but not $C_4$

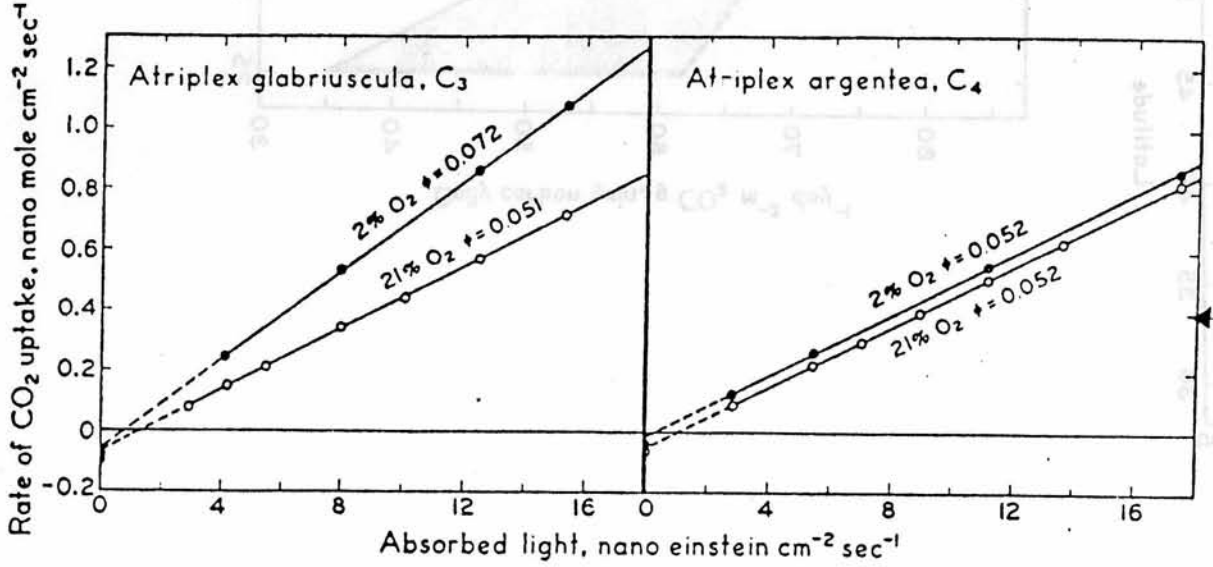


no difference in $C_4$ : independent of $[O_2]$

11

Minimum (January)

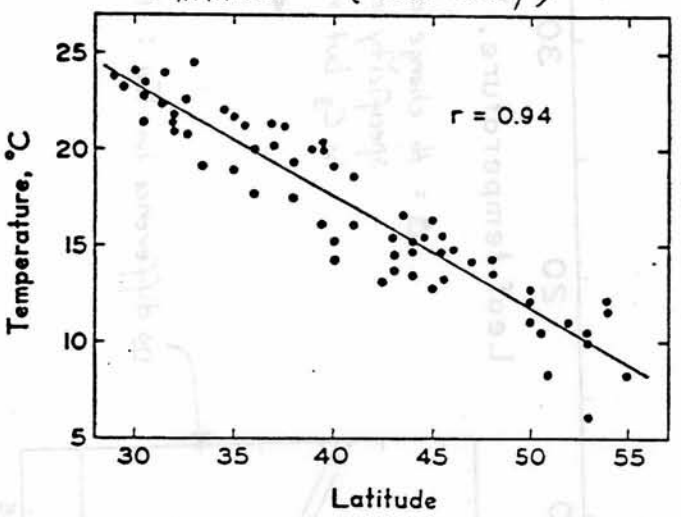


Maximum (July)

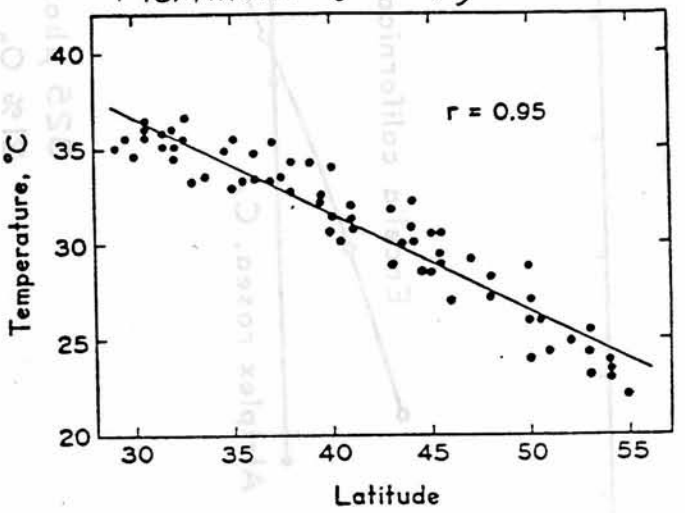


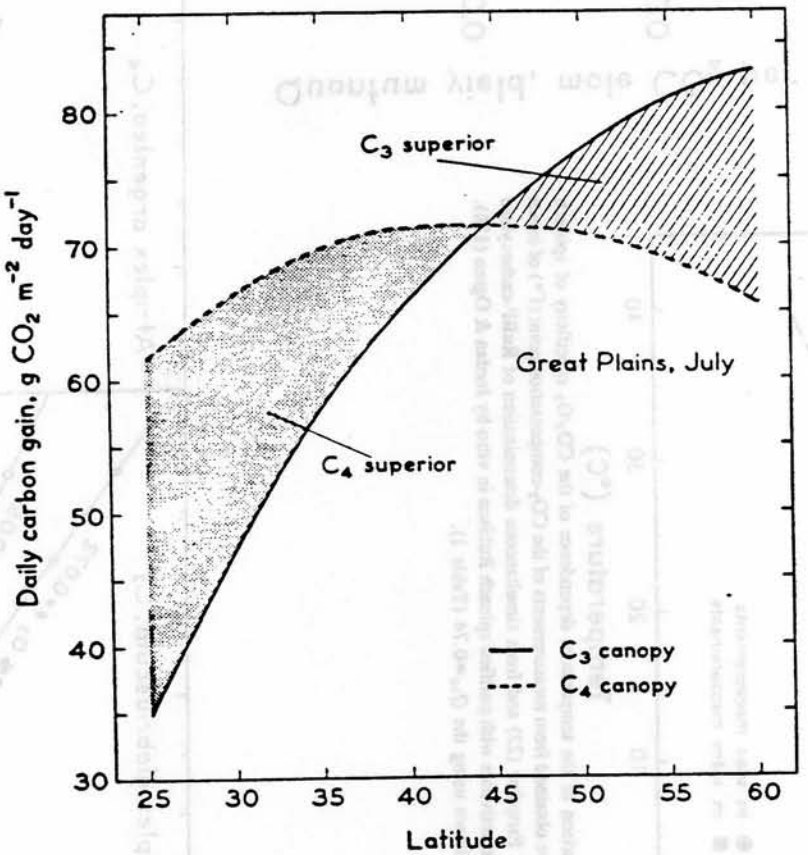

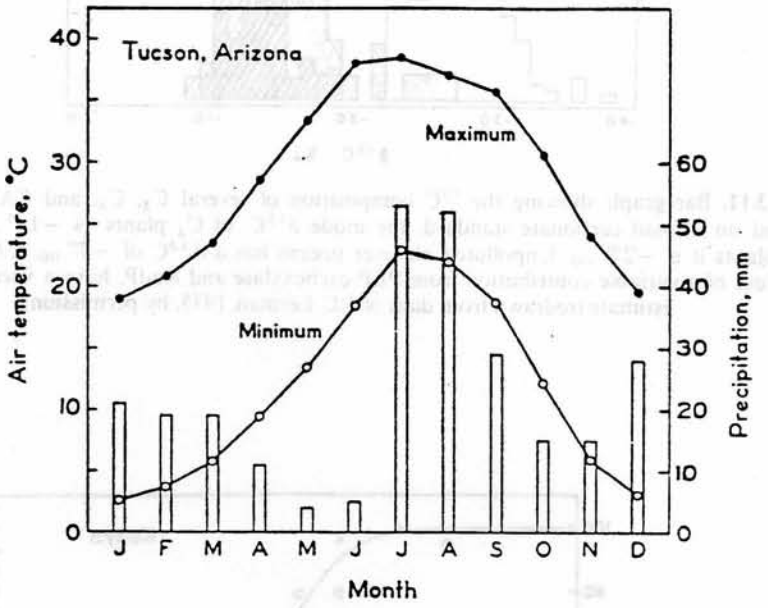
Tucson, Arizona
Maximum
Minimum
Air temperature, °C
Precipitation, mm
Month
J F M A M J J A S O N D
0 10 20 30 40
0 10 20 30 40 50 60

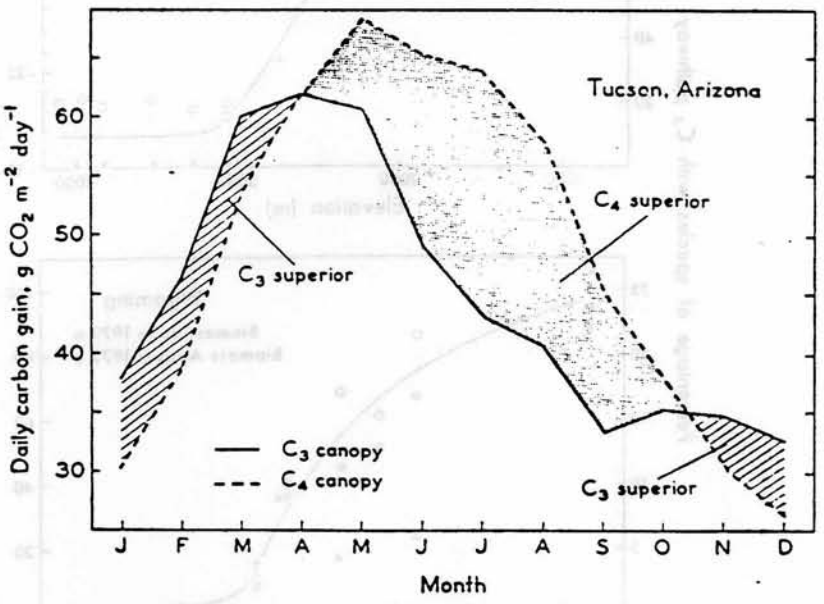
Tucson, Arizona
C4 superior
C3 superior
C3 canopy
C4 canopy
C3 superior
Daily carbon gain, g CO2 m-2 day-1
Month
J F M A M J J A S O N D
30 40 50 60

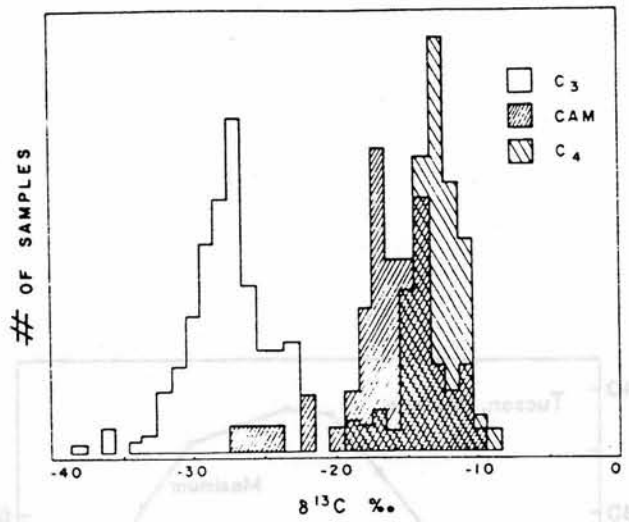


**Fig. 3.11.** Bar graph showing the $^{13}C$ composition of several $C_3$, $C_4$, and CAM species. Based on a fossil carbonate standard, the mode $\delta^{13}C$ of $C_4$ plants is $-11^{0}/_{00}$ and for $C_3$ plants it is $-27^{0}/_{00}$. Unpolluted air over oceans has a $\delta^{13}C$ of $-7^{0}/_{00}$. CAM plants, because of a variable contribution from PEP carboxylase and RudP, have a variable $\delta^{13}C$ estimate (redrawn from data of J.C. Lerman, 1975, by permission)

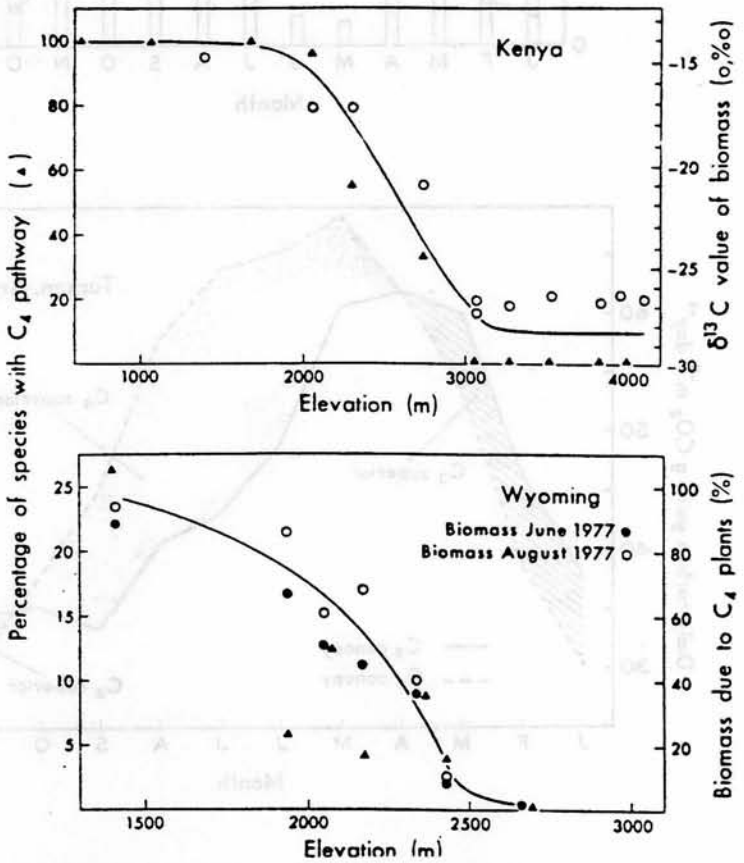


**Fig. 15.19.** Correlations between the percentage of taxa which are $C_4$ plants and the biomass due to $C_4$ plants for two grassland ecosystems. Contribution of $C_4$ plants to biomass was estimated by $\delta^{13}C$ value (Kenya) or by taxonomic evaluation (Wyoming). (Redrawn from data of TIESZEN et al. 1979; BOUTTON et al. 1980)

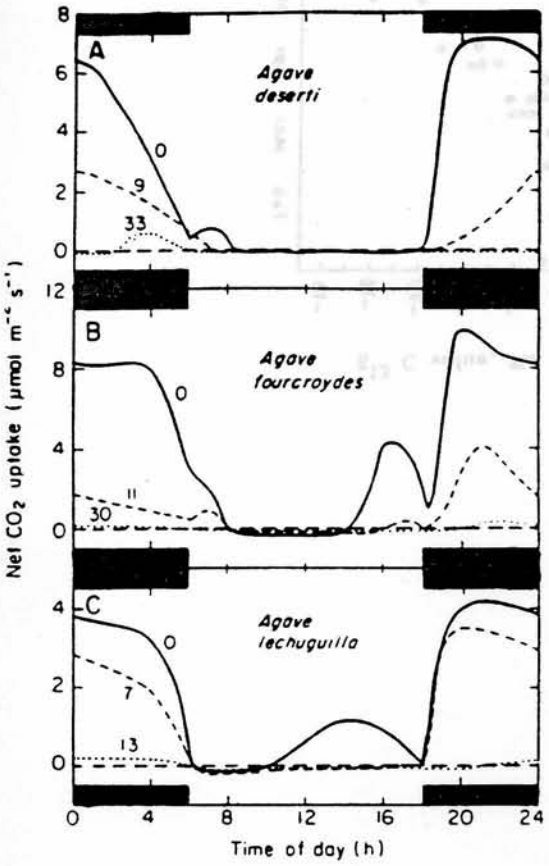


Figure 3.17. $CO_2$ exchange over a 24-h period by leaves of agaves after various periods of drought, indicated in days next to the curves. Data for (A) *Agave deserti* are adapted from Nobel (1984a), for (B) *A. fourcroydes* from Nobel (1985a), and for (C) *A. lechuguilla* from Nobel and Quero (1986). Gas exchange was measured in the laboratory under nearly saturating PAR, and the night temperature was constant at about the mean annual value of 15°C for *A. deserti*, 20°C for *A. fourcroydes*, and 9°C for *A. lechuguilla*.

numbers on the different lines represent the # of days since the plant received water.

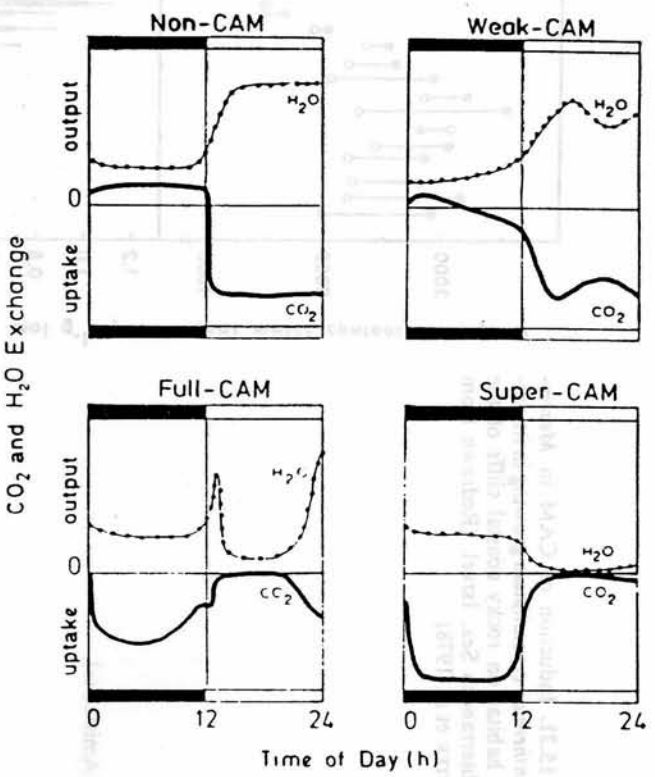


**Fig. 5.2.** Schemes of gas-exchange patterns as performed by CAM plants (after Neales, 1975, by permission)

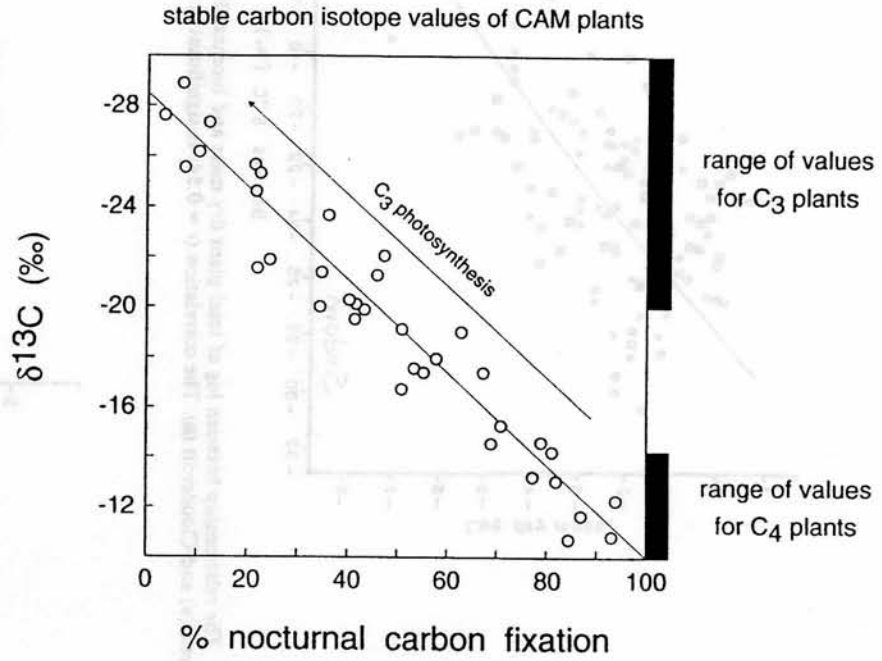

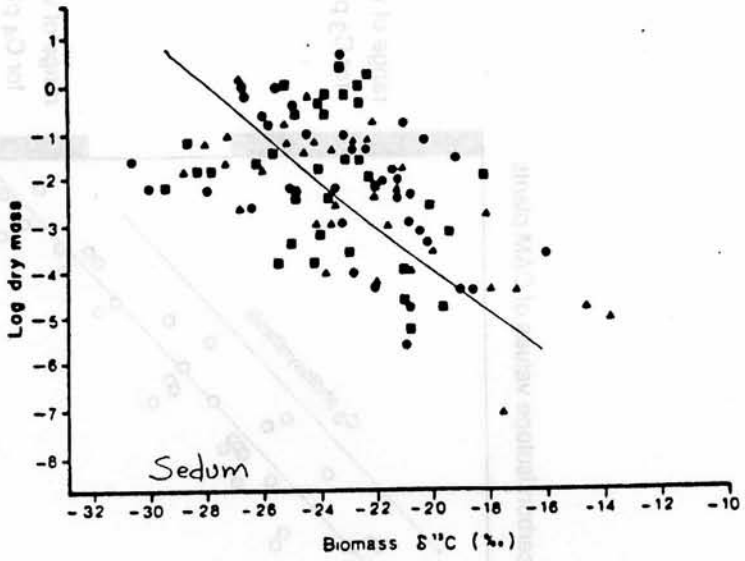


FIG. 3. The relationship between log of total plant dry mass and biomass $\delta^{13}C$ value for three populations: Amistad (▲), Fern Canyon (●) and Cloudcroft (■). The correlation ($r = 0.54$) is significant at the .0001 level.

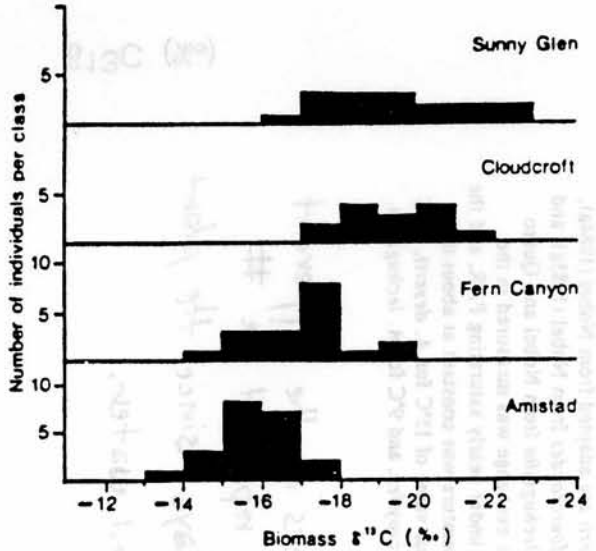


FIG. 2. Field biomass $\delta^{13}C$ values of the most recently expanded leaf from individuals of four populations of *Sedum wrightii*.

**Fig. 15.21.** Induction of CAM in *Mesembryanthemum crystallinum* growing in its natural habitat on rocky coastal cliffs of the Mediterranean Sea. Israel. (Redrawn from WINTER et al. 1978)

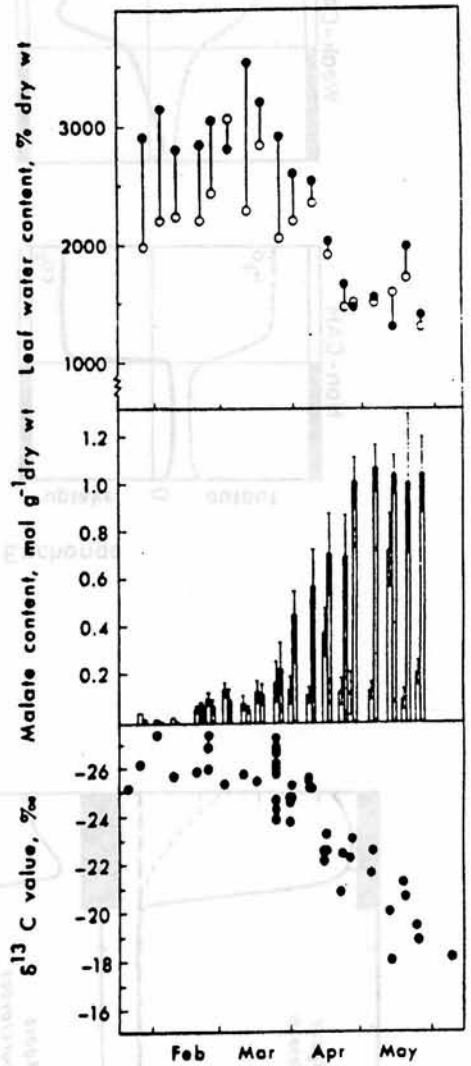

*Temporal variations in water availability*

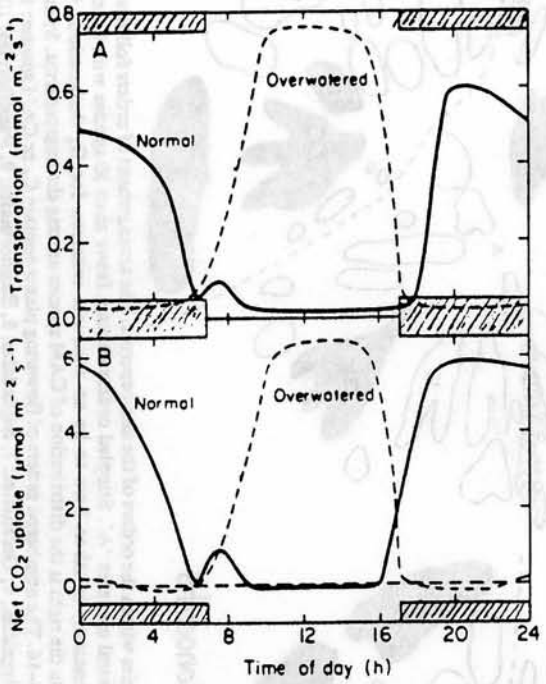


Figure 3.15. Influence of water status on (A) the daily pattern of transpiration and (B) net $CO_2$ uptake for *Agave deserti*. "Normal" refers to a plant receiving daily watering for two weeks, and "overwatered" refers to the same plant after an additional ten weeks of daily watering. Modified from Hartsock and Nobel (1976).

A response that on happens in leaf-succulent CAM plants; not in stem-succulent taxa

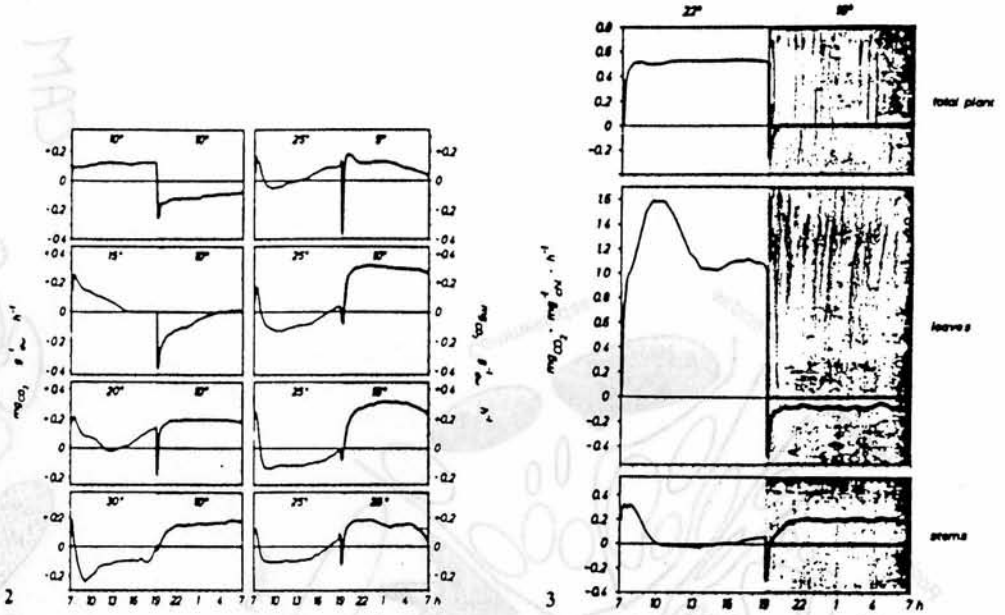

Fig. 2. Diurnal courses of $CO_2$ exchange (related to g dry weight) of leafless stems of *Frerea indica* in its winter state of development at different temperature conditions. Dark period indicated by shading

Fig. 3. Diurnal courses of $CO_2$ exchange (related to mg chlorophyll content) of leaf bearing intact plants of *Frerea indica* in its summer state of development (*top*), of cut off leaves (*middle*) and of defoliated stems (*bottom*). 22° C day and 10° C night temperature, dark period indicated by shading

A Stem Succulent CAM Plant with Deciduous $C_3$ Leaves

Table 1. Diurnal $CO_2$ gain (mg $CO_2$ per g dry weight) of *Frerea indica* in its summer state of development (conditions as indicated in Fig. 3)

| | 12 h light period | 12 h dark period | 24 h total |
|---|---|---|---|
| Total plants | + 34.86 | −0.66 | + 34.20 |
| Defoliated stems | + 0.53 | +1.79 | + 2.32 |
| Cut off leaves | +114.40 | −8.10 | +106.30 |

17

C4

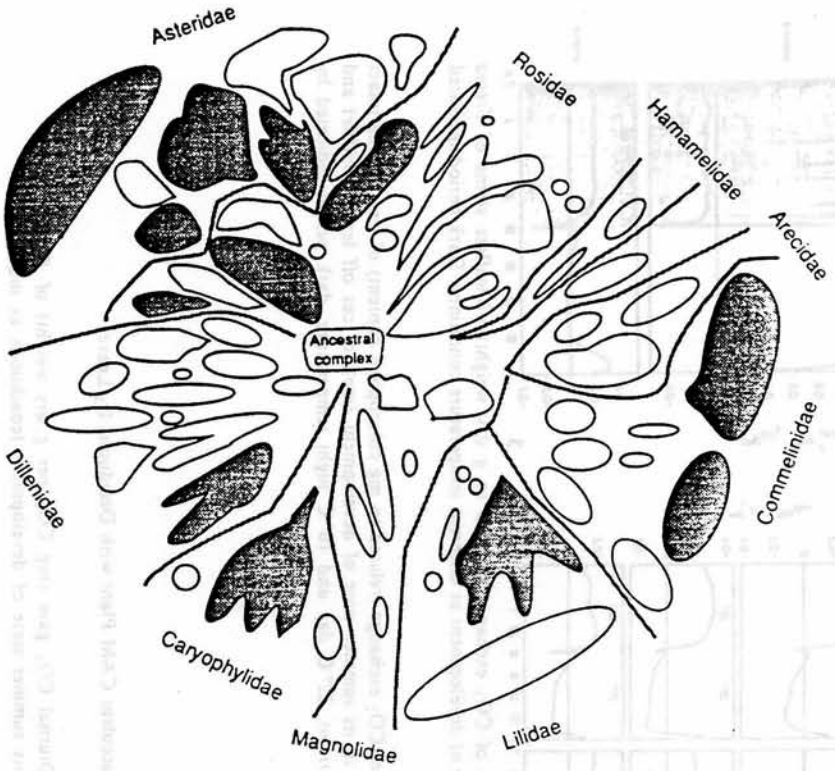


C4

CAM

Dicots

Monocots

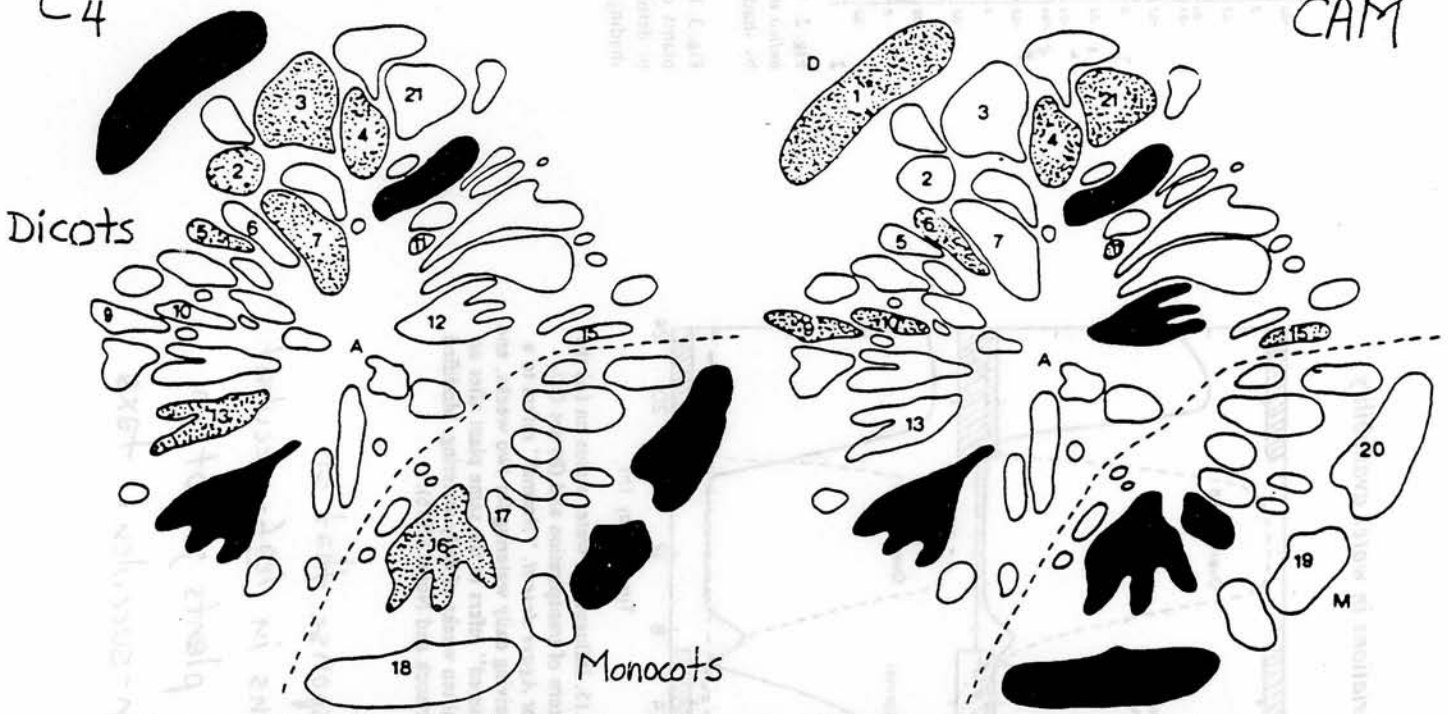


The diagram on the left shows the distribution of $C_4$ species within the orders of the angiosperms. The arrangement of orders follows Stebbins[12], in which they are shown to radiate from a proposed ancestral complex 'A'. Stippled orders contain fewer than 30 species with $C_4$ characteristics, shaded orders contain more than 30 species. Kranz anatomy is taken here to be an adequate criterion for $C_4$ designation, which may be questionable[9]. D, dicotyledons; M, monocotyledons. On the right is the distribution of CAM species among the angiosperms. Symbols as above. The data given in both diagrams are derived from refs 13–16. The numbered orders of flowering plants contain $C_4$ or CAM species: 1, Asterales; 2, Polemoniales; 3, Scrophulariales; 4, Gentianales; 5, Polygalales; 6, Geraniales; 7, Sapindales; 8, Euphorbiales; 9, Passiflorales; 10, Violales; 11, Rhamnales; 12, Rosales; 13, Capparales; 14, Caryophyllales; 15, Piperales; 16, Liliales; 17, Bromeliales; 18, Orchidales; 19, Cyperales; 20, Poales (Gramineae); 21, Lamiales.

Stippled areas = orders with < 30 species

Black areas = orders with > 30 species

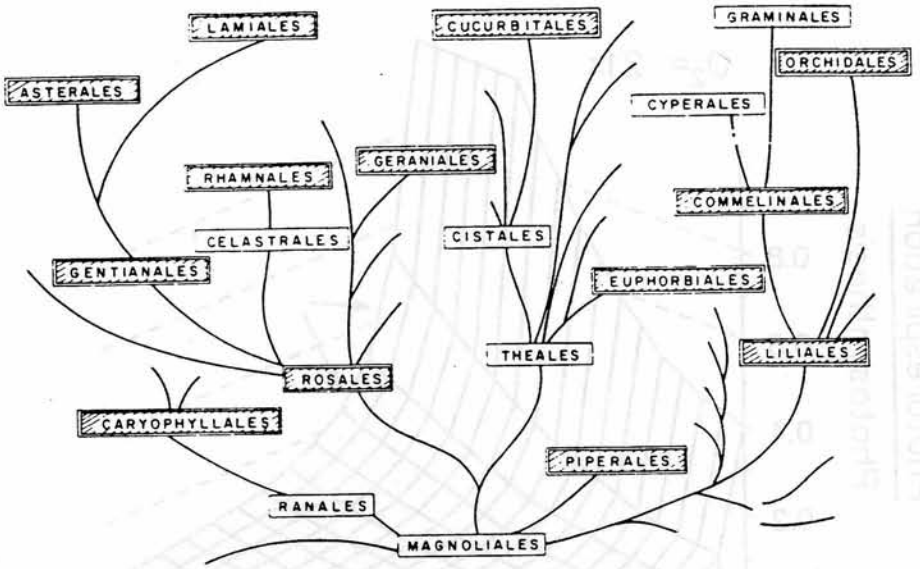


**Fig. 1.1.** Modified phylogenetic tree showing distribution of CAM families within orders. Tree drawn after Taktajan (1969). *Asterales* (Asteraceae): *Caryophyllales* (Aizoaceae, Cactaceae, Didiericeae, Portulacaceae): *Commelinales* (Bromeliaceae): *Cucurbitales* (Cucurbitaceae): *Euphorbiales* (Euphorbiaceae): *Gentianales* (Asclepiadaceae): *Geranales* (Geraniaceae, Oxiladaceae): *Lamiales* (Labiatae): *Liliales* (Agavaceae, Liliaceae): *Orchidales* (Orchidaceae): *Piperales* (Piperaceae): *Rhamnales* (Vitaceae): *Rosales* (Crassulaceae)

## Taxonomy and Geographical Distribution of CAM Plants

Table 1.1. Flowering plant families known to have species showing CAM

| | |
|---|---|
| Agavaceae | Euphorbiaceae |
| Aizoaceae | Geraniaceae |
| Asclepiadaceae | Labiatae |
| Asteraceae | Liliaceae |
| Bromeliaceae | Oxalidaceae |
| Cactaceae | Orchidaceae |
| Crassulaceae | Piperaceae |
| Cucurbitaceae | Portulacaceae |
| Didieraceae | Vitaceae |

Proposed Evolutionary Sequence From $C_3$ to $C_4$

| | $C_3$ | | | $C_4$ |
|---|---|---|---|---|
| Evolutionary Modification | Increased concentration of organelles in BSCs and differential compartmentation of glycine and decarboxylase between MC and BSC | Increased PEP carboxylase activity in both MC and BSC | Increased expression of $C_4$ biochemical steps in both MC and BSC | Differential compartmentation of $C_3$ and $C_4$ biochemistry between BSC and MC |
| Advantage of Evolutionary Modification | Increased efficiency of refixing photorespired $CO_2$ without impairing mesophyll assimilation of atmospheric $CO_2$ | Increased trapping of photorespired $CO_2$ before it escapes from the cell | Processing of $C_4$ products produced from PEP carboxylation and supply of PEP substrate to PEP carboxylase | $CO_2$-concentrating function and improved photosynthetic water- and nitrogen-use efficiencies |
| Representative Species at Their Respective Ranks | *Parthenium hysterophorus*<br>*Alternanthera ficoides*<br>*Alternanthera tenella* | *Flaveria linearis*<br>*Moricandia arvensis*<br>*Panicum milioides*<br>*Mollugo verticillata* | *Flaveria pubescens*<br>*Flaveria floridana*<br>*Flaveria anomala*<br>*Flaveria ramosissima*<br>*Neurachne minor* | *Flaveria brownii*<br>*Flaveria palmeri* |

Fig. 5. An evolutionary scheme to explain the steps taken during the evolution of $C_4$ plants from $C_3$ plants. Representative $C_3$–$C_4$ intermediates are presented at their respective positions along the proposed evolutionary sequence. Not all of the proposed evolutionary traits have been described for the species listed under that trait. For example, the presence of differential compartmentation of glycine decarboxylase has only been reported for two species. *Flaveria ramosissima* and *Moricandia arvensis*.

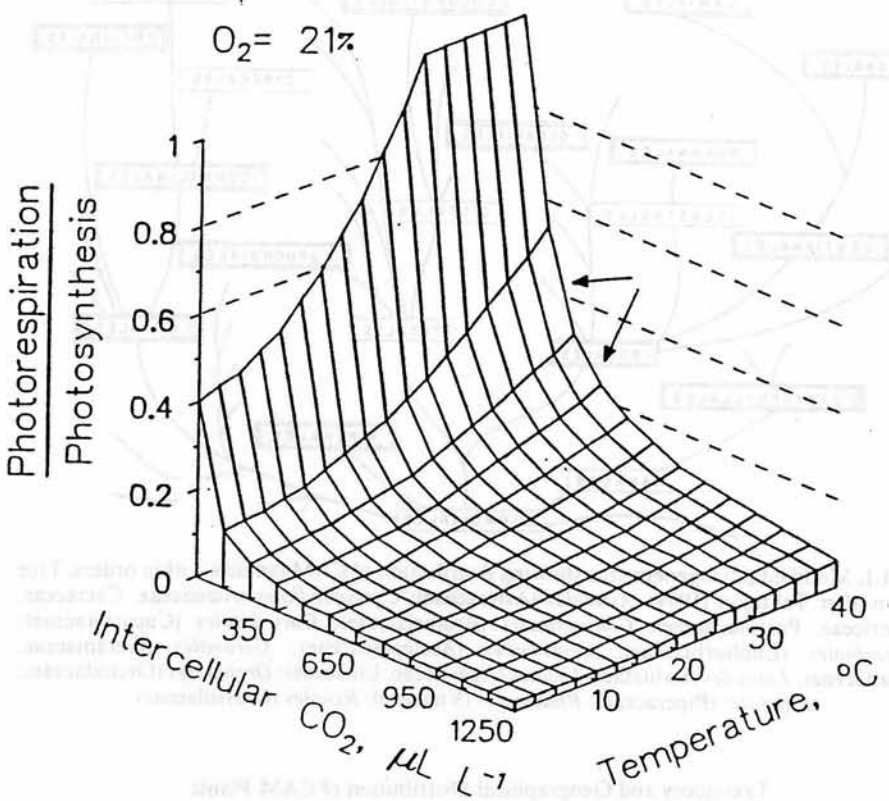


The Ratio of Photorespiration to Photosynthesis as a Function of Temperature and $CO_2$

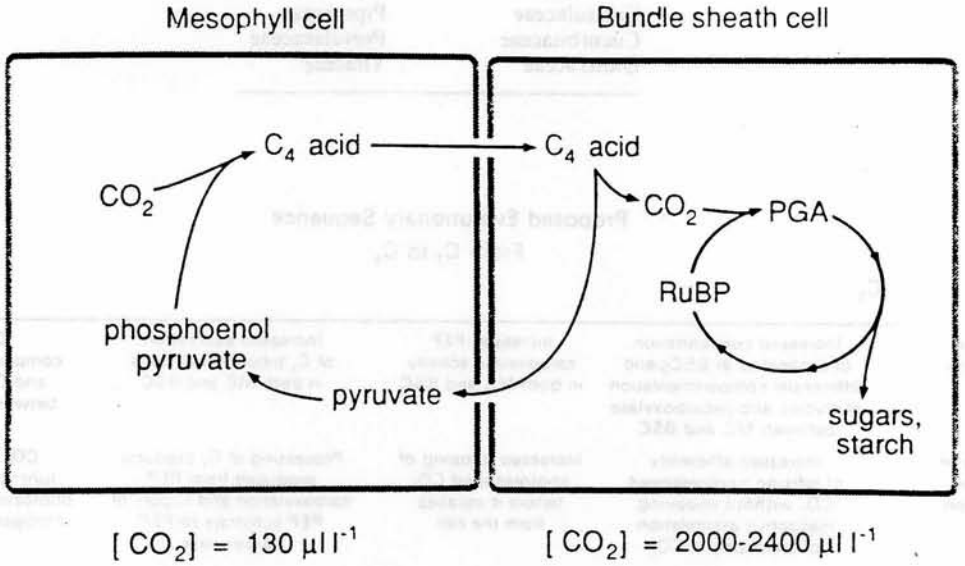


**Fig. 2.** Diagrammatic representation of $C_4$ photosynthesis. Atmospheric carbon is initially fixed inside leaf mesophyll cells in a reaction catalysed by phosphoenol pyruvate (PEP) carboxylase. The resulting $C_4$ acid is decarboxylated inside the bundle sheath cell, providing a source of $CO_2$ for ribulose-1,5-bisphosphate carboxylase (Rubisco) and the normal $C_3$ photosynthetic cycle. $C_4$ photosynthesis acts as a $CO_2$-concentrating mechanism. The $CO_2$ concentration inside the bundle sheath, where Rubisco functions, is 10- to 20-fold higher than the $CO_2$ concentration in the leaf mesophyll cells. PGA, phosphoglycerate; RuBP, ribulose bisphosphate.

from: Ehleringer et. al., 1991

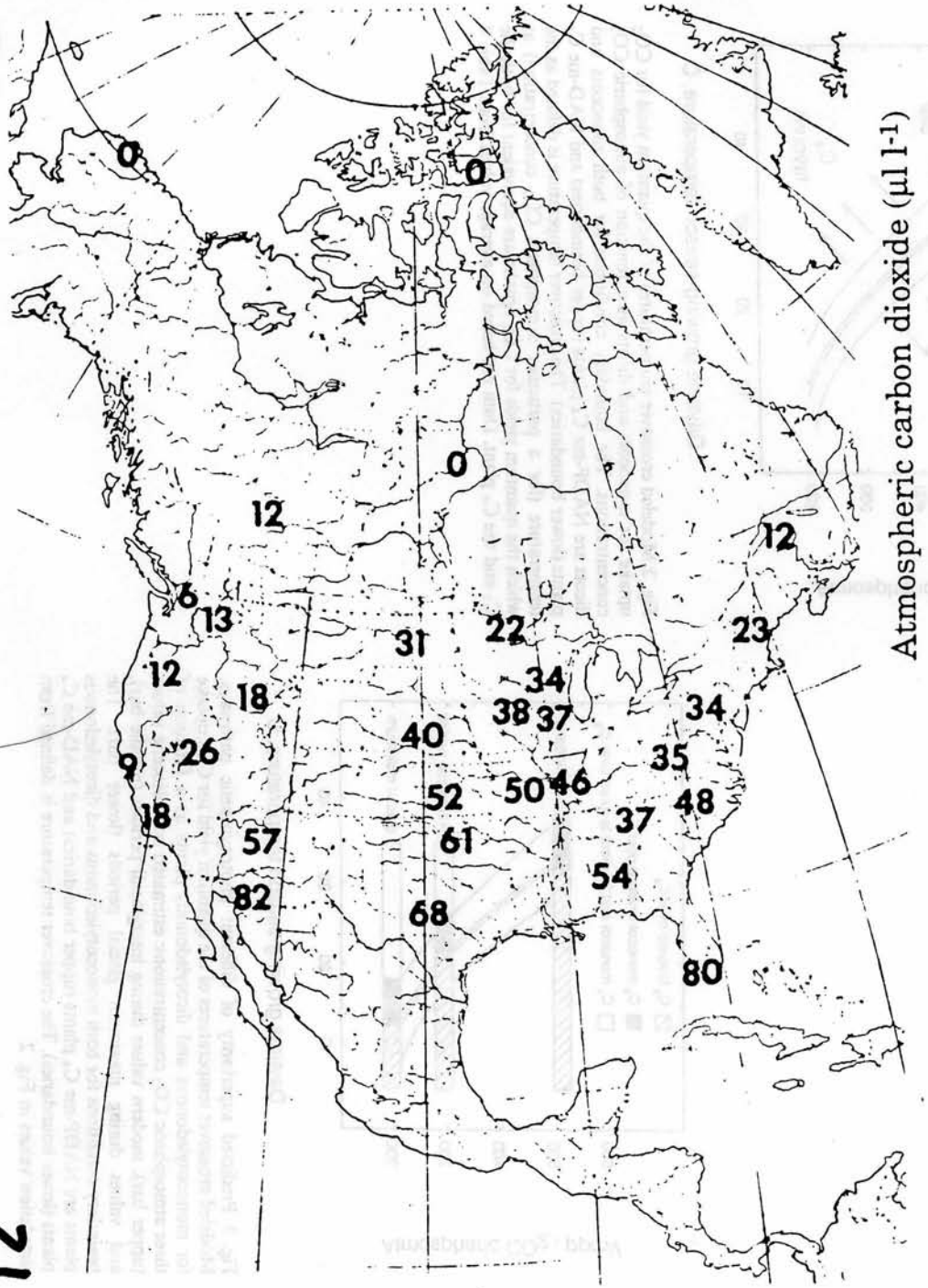


from: Teevi & Stowe (1976)

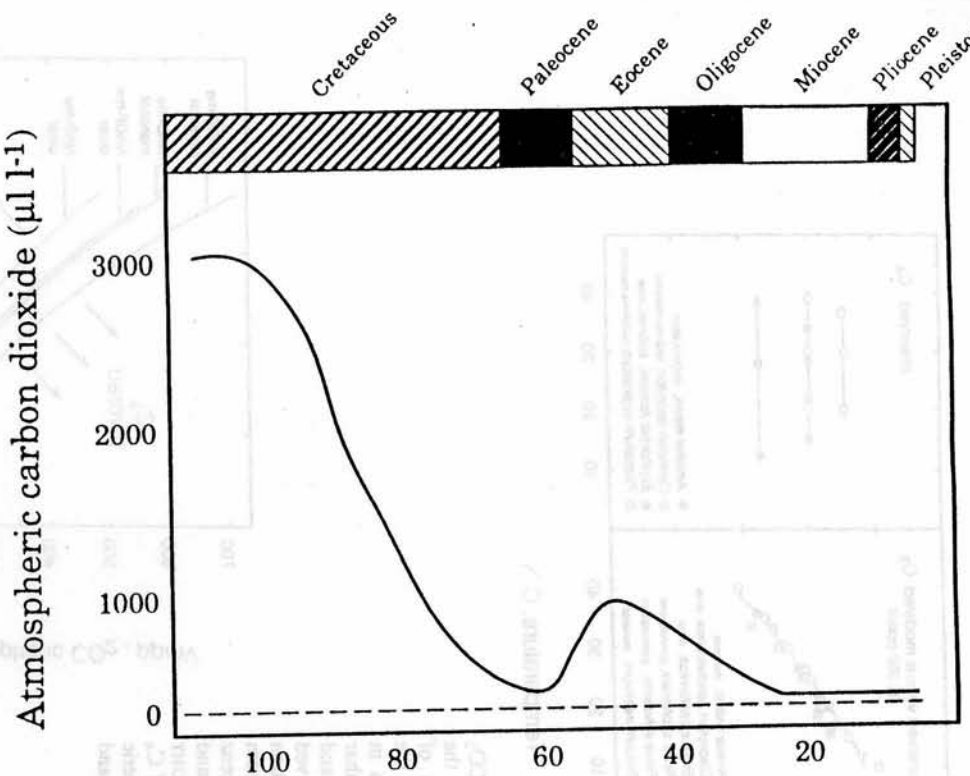


from: Ehleringer et al. 1991

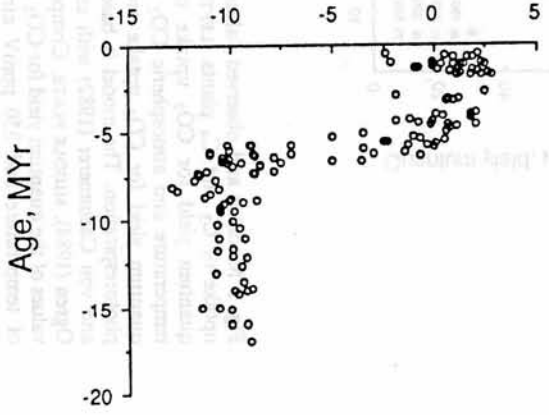

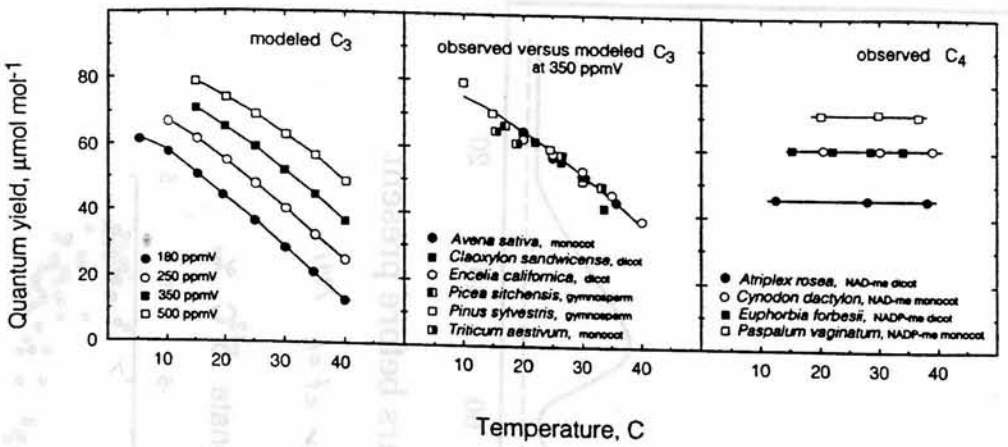


**Fig. 1** Modeled and observed values of the quantum yield for $CO_2$ uptake of $C_3$ and $C_4$ plants. LEFT PLATE. Modeled values of the quantum yield for $CO_2$ uptake of $C_3$ plants as a function of temperature and atmospheric $CO_2$ concentrations. Changes in the quantum yield for $CO_2$ uptake are largely driven by changes in photorespiration. The model is based on equations from Farquhar and von Caemmerer (1982) with enzymatic data from Jordan and Ogren (1984). MIDDLE PLATE. Comparison of modeled and observed values of the quantum yield for $CO_2$ uptake of $C_3$ plants as a function of temperature and 350 ppmV atmospheric $CO_2$. Data are from Ehleringer and Björkman (1977), Ku and Edwards (1978), Leverenz and Jarvis (1979), Robichaux and Pearcy (1980), Ehleringer and Pearcy (1983), Öquist and Strand (1986), and Wang (1996). RIGHT PLATE. Observed values of the quantum yield for $CO_2$ uptake of $C_4$ plants as a function of temperature and 320–340 ppmV atmospheric $CO_2$. Data are from Ehleringer and Björkman (1977), Robichaux and Pearcy (1980), and Ehleringer and Pearcy (1983)

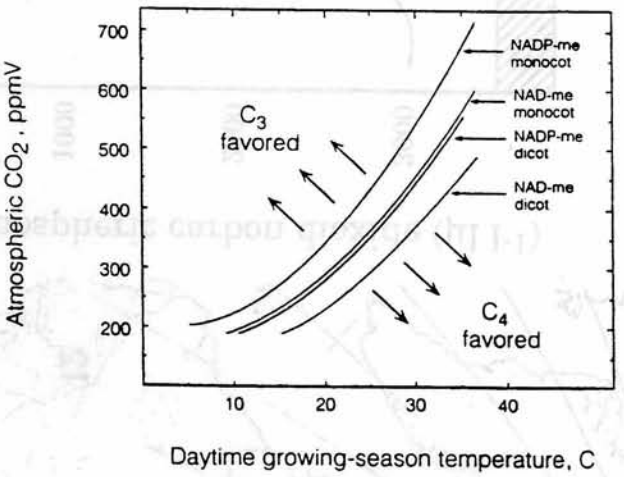


**Fig. 2** Modeled crossover temperatures of the quantum yield for $CO_2$ uptake for monocots and dicots as a function of atmospheric $CO_2$ concentrations. The boundary conditions for both monocots and dicots are NADP-me $C_4$ plants (upper boundaries) and NAD-me $C_4$ plants (lower boundaries). The crossover temperature is defined as the temperature (for a particular atmospheric $CO_2$ concentration) at which the quantum yields for $CO_2$ uptake are equivalent for both the $C_3$ and the $C_4$ plant. Data are based on average values from Table 4

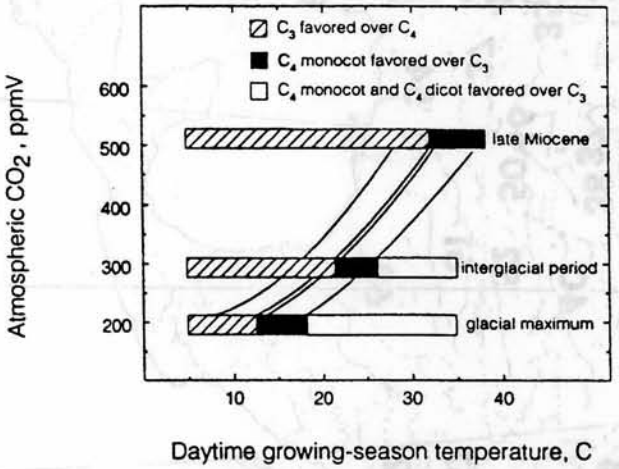


**Fig. 3** Predicted superiority of different photosynthetic pathways. Modeled crossover temperatures of the quantum yield for $CO_2$ uptake for monocotyledonous and dicotyledonous plants as a function of three atmospheric $CO_2$ concentrations: estimated late Miocene values (upper bar), modern values during interglacial periods (middle bar), and values during maximum glacial periods (lower bar). The boundary conditions for both monocotyledonous and dicotyledonous plants are NADP-me $C_4$ plants (upper boundaries) and NAD-me $C_4$ plants (lower boundaries). The crossover temperature is defined from simulation values in Fig. 2